Food Structure

Volume 4 | Number 1 Article 17

1985

Ultrastructural Studies on the Cultivation Processes and Growth and Development of the Cultivated Mushroom Agaricus Bisporus

D. A. Wood

G. D. Craig

P. T. Atkey

R. J. Newsam

K. Gull

FOOD MICROSTRUCTURE, Vol. 4 (1985), pp. 143-164
SEM Inc., AMF O'Hare (Chicago), IL 60666-0507 U.S.A.

0730-5419/85$1.00+.05

ULTRASTRUCTURAL STUDIES ON THE CULTIVATION PROCESSES AND GROWTH AND DEVELOPMENT OF THE CULTIVATED MUSHROOM *AGARICUS BISPORUS*

D.A. Wood[1]*, G.D. Craig[2], P.T. Atkey[1], R.J. Newsam[3] and K. Gull[3]

[1] Dept. of Plant Pathology & Microbiology, Glasshouse Crops Research Institute, Littlehampton, West Sussex, BN17 6LP, UK
[2] Dept. of Life Sciences, Nottingham Polytechnic, Nottingham, UK
[3] Biological Laboratory, University of Kent, Canterbury, Kent, UK

Abstract

Scanning electron microscopy (SEM), transmission electron microscopy and light microscopy have been used to study various processes in the cultivation of the edible mushroom Agaricus bisporus. Mushrooms are cultured on composted wheat straw. The microbial degradation processes during composting have been visualised by TEM and SEM and correlated with microbiological studies. Various modes of attack by the microorganisms on the plant cell walls can be seen. Most rapid degradation occurred on the cuticle and phloem and spread to other cell types. Microbial attack was found to be non-uniform between tissue types and individual cells. The mycelium of Agaricus bisporus colonised the compost straw surface and the lumen of straw cells, and also degraded microbial cells therein.

The cellular organisation and ultrastructure of the rhizomorphs and of the developing stipe and gill tissue were examined. The development and branching patterns of the hyphae generating the sub-hymenium and hymenium layers of the gill tissue were examined. Light and electron microscope autoradiography were used to locate the site of synthesis of cell wall chitin and to demonstrate evidence for cell division in the upper stipe region.

Initial paper received February 18, 1985.
Final manuscript received May 21, 1985.
Direct inquiries to D.A. Wood.
Telephone number: (0903) 716123.

Key Words: mushroom, Agaricus, scanning electron microscopy, transmission electron microscopy, ultrastructure, compost, growth, development, autoradiography, cell division.

Introduction

The production of the cultivated mushroom is carried out on a large scale in North America, Europe, Australasia and parts of Asia. World production now exceeds 1.0 million tonnes per annum. Production is carried out by growing the mycelium of the fungus in composted substrates, such as manure-straw mixtures, and then harvesting the mushroom fruit bodies prior to marketing (Wood, 1984, Wood et al., 1984). In the United Kingdom the consumer preference is for fresh mushrooms but in North America, France and Asia considerable quantitites of mushrooms are canned before marketing.

Many microbiological studies have been carried out on the composting process used for the growth substrate on which mushrooms are cultivated (Fermor and Wood, 1979). A large and taxonomically diverse microbial flora has been shown to be involved in composting. These microbes include bacteria, actinomycetes and fungi and both mesophilic and thermophilic microbial groups are found. The soluble materials and certain of the insoluble materials of the substrate are utilised during composting (Fermor and Wood, 1979, Fermor and Wood, 1981).

After composting, the growth substrate (compost) is inoculated with mushroom mycelium and the compost is subsequently extensively colonised by the mycelium. Mushrooms arise as small knots or aggregates of hyphal cells and differentiate into the 3 tissue types of the mature structure, stipe, cap and gills.

We investigated the ultrastructure of the composting process and colonisation stages of mushroom production to determine the organisation and mode of attack of the microorganisms in the compost and to study the colonisation by the hyphae of the mushroom into the substrate. The development of the mushroom from the earliest stages to mature fruit bodies was examined by transmission electron microscopy (TEM) and scanning electron microscopy (SEM). Autoradiographic techniques were used to examine cell division and chitin synthesis in stipe tissue of the mushrooms.

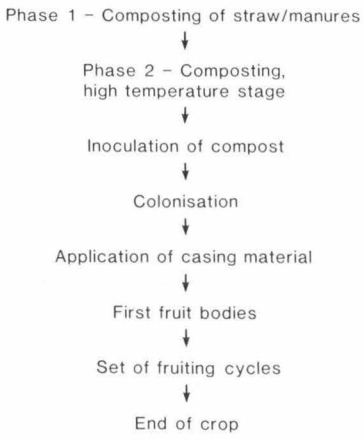

Fig. 1 A simplified schematic flow chart of the main stages in mushroom cultivation

Fig. 4 Day 0. SEM of raw straw surface. Note silica bodies (arrows). Bar 50 μm.
Fig. 5 Day 0. SEM of straw surface from stable manure. Note diverse microbial population. Bar 50 μm.
Fig. 6 Day 0. SEM of cut end of straw internode from stable manure showing microbial concentration in phloem. Bar 50 μm.
Fig. 7 Day 7. TEM of variety of microorganisms within a straw cell. Bar 2.5 μm.
Fig. 8 Day 7. TEM of straw showing absence of microbial colonisation. Bar 5 μm.
Fig. 9 Day 7. SEM of colony of coccoid bacterial cells on the straw surface. Bar 5 μm.
Fig. 10 Day 7. SEM of microorganisms on straw cuticle. Note erosion around silica body (arrow). Bar 25 μm.
Fig. 11 Day 14. TEM of bacteria within straw cells. Note erosion (W, cell wall) and glycocalyx material anchoring bacteria (g). Bar 1 μm.

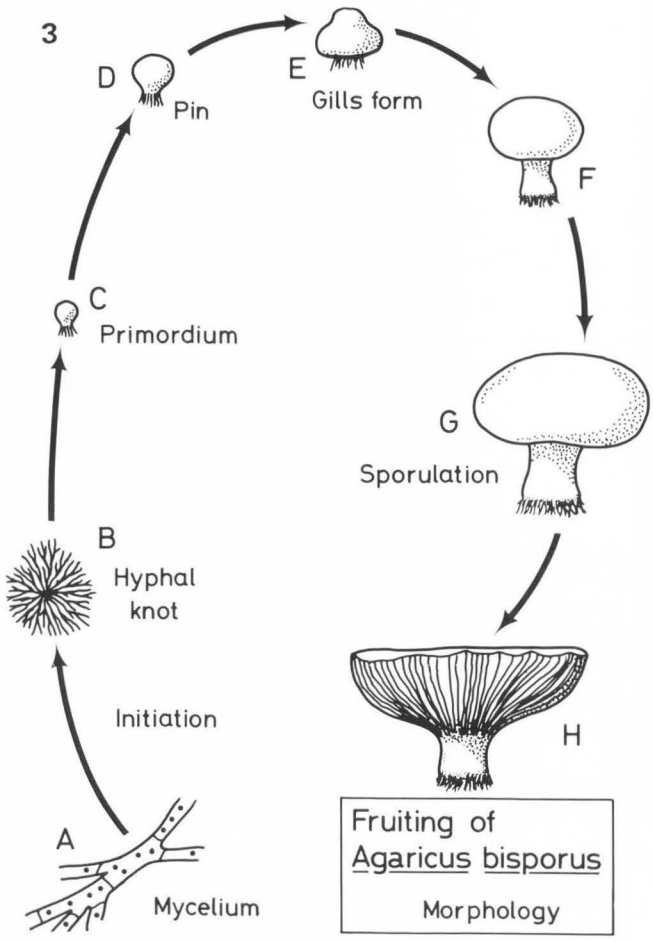

Fig. 3 Diagram of morphogenesis of the mushroom Agaricus bisporus

Fig. 2 Diagram of growth and cropping of the edible mushroom Agaricus bisporus on composted substrates

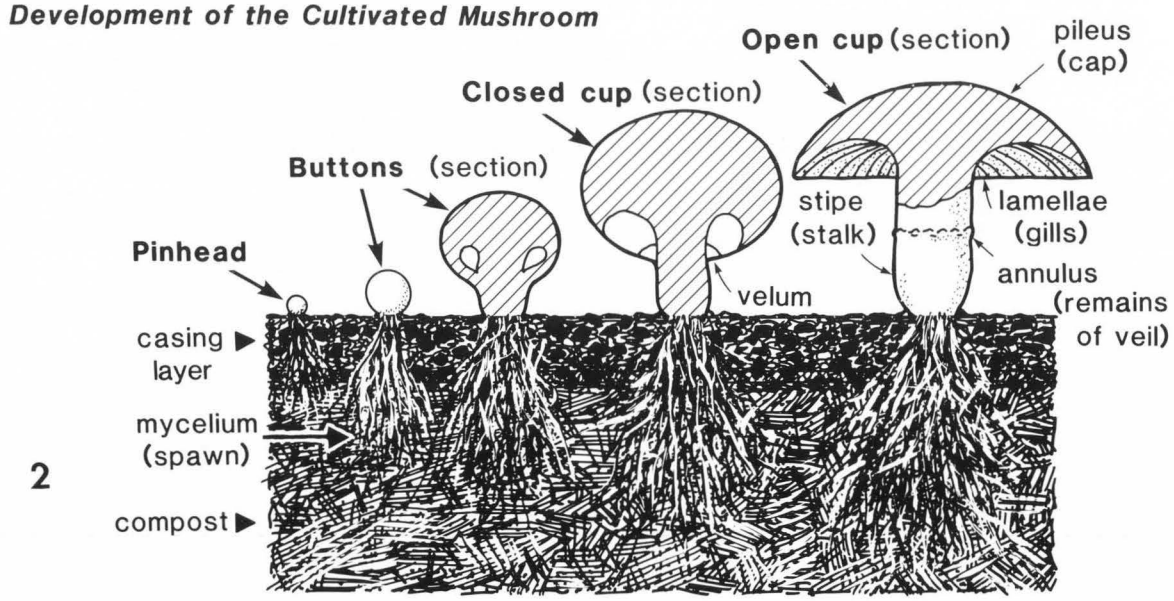

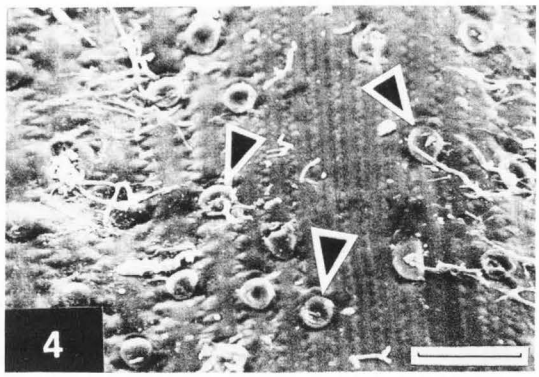
4

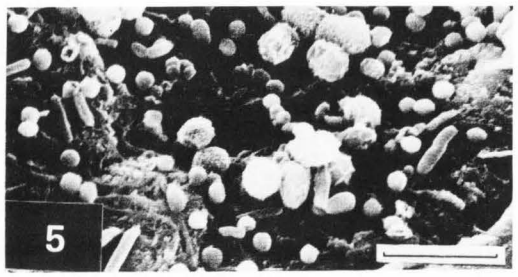
5

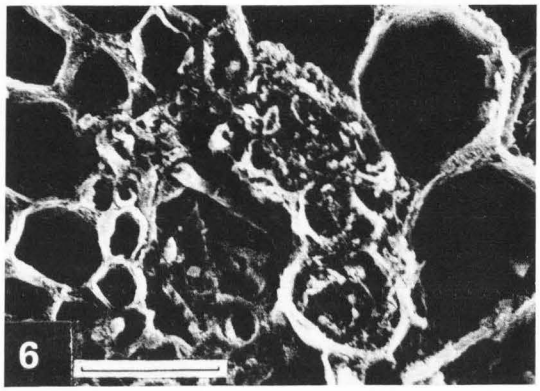
6


7

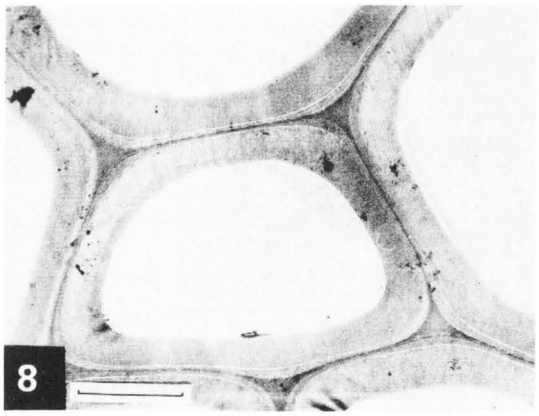
8

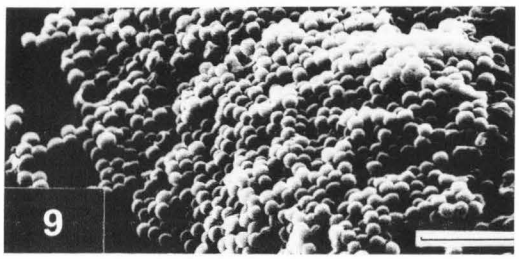
9

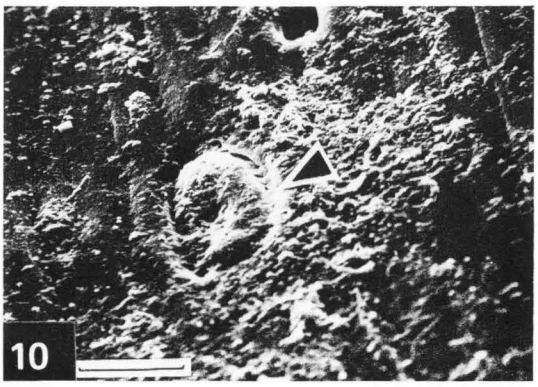
10


g
g
g
11

Materials and Methods

Samples from mushroom cultivation processes

A schematic flow chart of the major steps in mushroom cultivation is shown in Figure 1. A more detailed description of the process and the environmental and cultural parameters controlling it and their purpose can be found in Wood (1984). A summary of the growing procedure for mushrooms is shown in Fig. 2. Samples of straw internode material were taken from the bulk of the compost at each of the following stages of the cultivation process. Raw straw ± stable manure at 0 d, first phase of composting at 7 d, pasteurization at 14 d; mycelial inoculation at 21 d, application of casing material at 35 d, first appearance of fruit bodies at 56 d and end of fruiting at 112 d.

Transmission electron microscopy (TEM) of straw samples

Pieces of tissue ca 0.5 mm x 2 mm were cut from the internode region of the straw. These were fixed for 2 h in Karnovsky's fixative (Karnovsky, 1965) using half strength para-formaldehyde. Samples were fixed in embedding tubes as described by Pegler and Atkey (1978). The tissues were thoroughly rinsed in 0.2 M sodium cacodylate buffer pH 7.2; and post-fixed for 2 h in 2% osmium tetroxide. The tissue was then washed and dehydrated through a graded ethanol series and embedded in Spurr's resin (Spurr, 1969) after infiltration at 24 h for 3 increasing concentrations and a final 48 h in 100% resin. Fixation and dehydration was carried out at room temperature. Sections were cut with an LKB Ultratome III using glass knives, and then stained with aqueous uranyl acetate for 30 minutes and post-stained with Reynolds lead citrate solution (Reynolds, 1963) and examined in a JSM 100 S transmission microscope at 80 kV accelerating voltage.

Scanning electron microscopy (SEM) of straw samples

Straw internode tissue samples were fixed overnight at room temperature in 6% glutaralde-hyde buffered at pH 7.2 with 0.2 M sodium cacodylate. They were dehydrated by two immersions of 30 minutes in 100% 2-methy-oxyethanol followed by two washes in 100% acetone (Polak-Vogelzang et al., 1979). The specimens were then transferred to liquid carbon dioxide and dried in a Samdri-780 critical point drier. Specimens were then coated with gold/palladium in an EMSCope sputter coater and examined in a JEOL T20 scanning microscope at 20 kV accelerating voltage.

Samples from mushroom tissue

A diagram of the morphogenesis of *Agaricus bisporus* is shown in Figure 3. Samples for microscopy were taken from stages C, E, F, G.

Light microscopy

Small pieces of stipe tissue were removed at stages F and G, and fixed in 2.5% glutaraldehyde in sodium cacodylate pH 7.4. The samples were post fixed in 1% osmium tetroxide in veronal-acetate buffer pH 7.2 and then dehydrated in an ethanol series and embedded in Spurr's resin (Spurr, 1969). The tissue was embedded so longitudinal sections could be cut to reveal the orientation of the hyphae. Sections (0.5 µm) were cut with glass knives with a Reichert OMU3 ultratome, stained with 1% toludine blue and examined in a Zeiss Universal light microscope.

TEM of mushroom tissue

Samples of the material embedded for light microscopy were sectioned as described above and then post-stained with uranyl acetate and lead citrate. The sections were examined in an AEI 801 transmission microscope at 60 kV accelerating voltage.

SEM of mushroom tissue

Longitudinal and transverse sections of stipe and gill tissue (5 mm^2) were removed and fixed for 18 h in 2.5% glutaraldehyde in sodium cacodylate pH 7.4. The specimens were dehydrated through a graded acetone series each at 30 minutes and finally into 100% acetone. The specimens were then critical point dried with liquid carbon dioxide with a Polaron model E300 drier. The dried samples were sputter coated with gold and viewed in a Cambridge S600 scanning microscope at 15 or 25 kV accelerating voltage.

Autoradiographic techniques

Radiolabelled N-acetyl-D-(1-^{3}H) glucosamine, (Amersham), total volume 80 µl, with specific activity of 5 Ci/mM was injected into the stipe of a fruit body with a Hamilton syringe in several small portions. Fruit bodies were injected prior to the stipe expansion stage (Bonner et al., 1956; Craig, 1979; Craig et al., 1977b). For light microscopy and one electron microscope method the tissue was fixed in 5% KOH after 30 minutes incorporation.

Fig. 12 Day 14. SEM of straw surface showing heavily eroded cuticle and collapse of many cells. Bar 100 µm.
Fig. 13 Day 14. TEM of section through straw cell wall to show bacteria tunnelling in primary and secondary thickening. Note glycocalyx (g) and intercellular space (i). Bar 3 µm.
Fig. 14 Day 14. TEM of actinomycete hyphae (arrows) within a straw cell. Bar 2 µm.
Fig. 15 Day 14. SEM of actinomycete hyphae (arrows) growing near smooth fungal spores on straw surface. Bar 100 µm.
Fig. 16 Day 14. SEM of middle lamella of straw separating into fibre due to microbial erosion. Bar 500 µm.
Fig. 17 Day 14. SEM of straw xylem vessel from which the primary wall has been eroded to reveal the secondary annular thickening as discrete rings. Note separated annulus (arrow). Bar 25 µm.
Fig. 18 Day 21. SEM of bacteria embedded in walls of straw cell. Bar 10 µm.
Fig. 19 Day 21. TEM of fungal spore (F) in straw cell. Note broken and disrupted cell walls (W). Bar 2 µm.

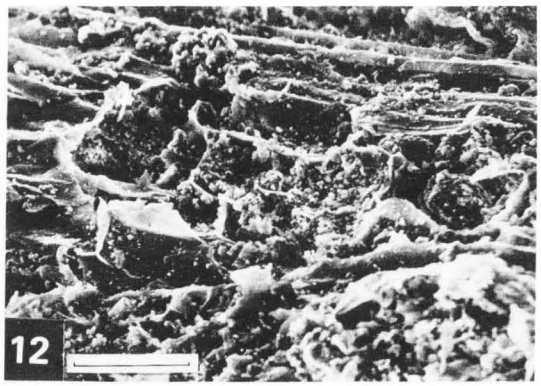
12

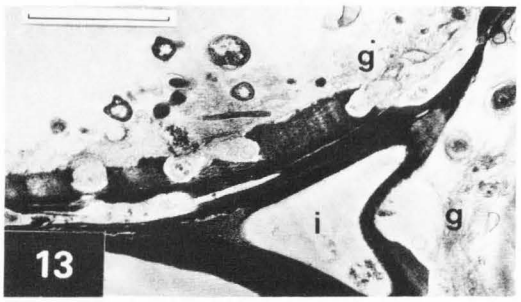
g
i
g
13

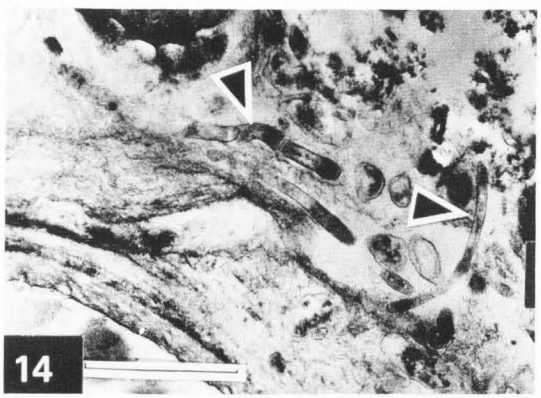
14

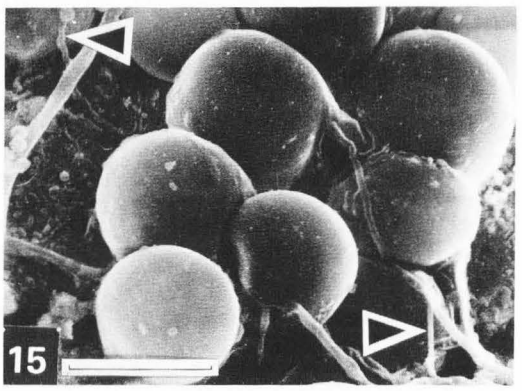
15

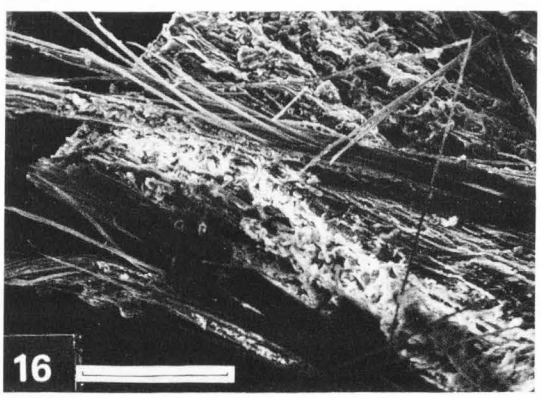
16

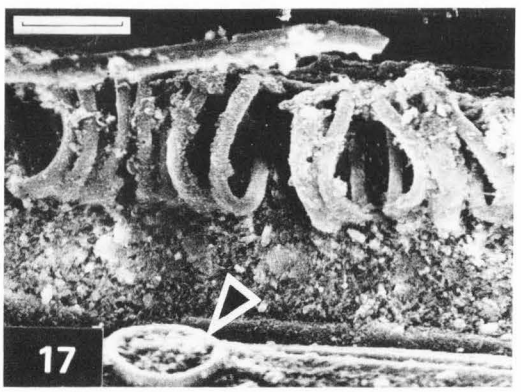
17

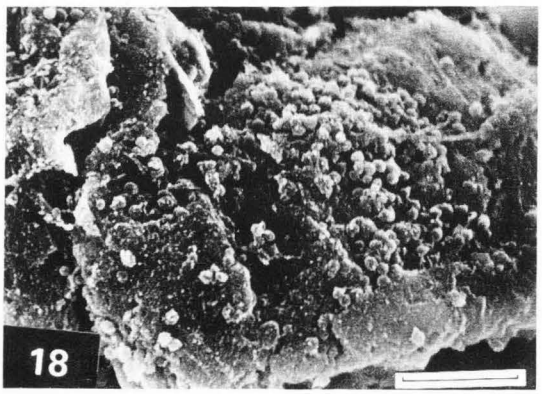
18

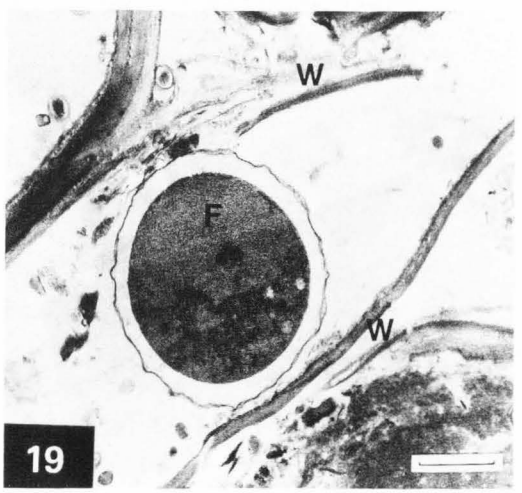
W
F
W
19

For light microscopy the cells of the stipe tissue were separated by shaking in 5% KOH on a wrist action shaker in the presence of glass beads. The separated hyphae were then washed in distilled water and stained with 5% Congo Red in 50% ethanol for 15 minutes. Kodak AR-10 was used as a medium for stripping film autoradiography. The film was exposed for 3 days at 4°C. The slides were developed in Kodak D-19 for 5 minutes and fixed in Kodak Unifix fixer. The slides were mounted in Depex mounting medium and examined in a Zeiss Universal microscope.

Two methods were used for electron microscope autoradiography. For the first method labelled cells separated as described above were placed on formvar/carbon coated 200 mesh coated grids. The cells were allowed to settle and excess liquid removed. The grids were then coated with Ilford L4 nuclear emulsion by a loop method (Caro et al., 1962). The sample was exposed for 1-2 weeks at 4°C. The second method was to embed labelled stipe material in Spurr's resin. Thin sections were cut with a diamond knife and placed on formvar/carbon grids. Emulsion was applied as above and exposed for 6 weeks. Grids were then developed in Kodak D-19, for 4 minutes, rinsed and then fixed in 20% sodium thiosulphate. The grids were examined in an AEl 801 transmission microscope at 60 kV accelerating voltage.

Results

Composting, Day 0

Straw prior to composting showed little microbial colonisation other than occasional groups of fungal spores near fractured surfaces. The surfaces of the straw had a sparse covering of scattered bacterial colonies and fungal hyphae. Some of this colonisation was associated with depressions in the straw epidermis termed silica bodies (Fig. 4). Straw premixed with stable manures contained a large morphologically diverse bacterial population (Fig. 5). Colonisation was widespread but variable on the straw surface but internally restricted to phloem tissue (Fig. 6). At this stage there was little erosion, other than phloem tissue, of internal straw cell walls.

Composting, Day 7

TEM and SEM examination revealed considerable microbial populations on (Fig. 7) and within the straw but the distribution of the colonisation was uneven. Certain straw cells contained dense mixed populations of bacteria (Fig. 7) but many contained few or no micro-organisms (Fig. 8). Colonies of coccoid bacteria were seen on the straw surface (Fig. 9) and actinomycetes and fungal spores were also present in low numbers. The overall integrity of the straw structure was altered little although erosion of the cuticle, particularly in the zones around the silicon bodies, was pronounced (Fig. 10).

Composting, Day 17 (Pasteurization)

By this stage dense bacterial populations were present both within and on the straw (Fig. 11). The erosion patterns produced by the bacteria included concave depressions in the plant wall secondary thickening (Fig. 11). The epidermal straw layers were heavily eroded leading to collapse of many cells (Fig. 12). Some erosion patterns showed as tunnelling along the thickening causing it to part from the middle lamella (Fig. 13). Actinomycete hyphae could be seen within the straw at this stage (Fig. 14) and also on the straw surface where they were associated with larger fungal spores (Fig. 15). In many cases erosion of the middle lamellae had advanced sufficiently to produce fibre separation (Fig. 16). In certain cases the primary xylem walls were destroyed leaving the more resistant secondary annular thickenings as discrete rings (Fig. 17).

Inoculation, Day 21

TEM showed that the numbers of bacteria were reduced with many more spore forms present. The bacteria were often embedded within the plant cell walls (Fig. 18). Fungal spores were present both on the surface and within the straw tissue (Figs. 19, 20). On the surface these spores were often covered with a mat of actinomycete hyphae (Fig. 20). The actinomycetes could be often seen to produce 'bud-like' branching in association with the plant cell wall (Figs. 21, 22). The straw tissue showed increasing damage with a greater proportion of collapsed cells (Figs. 21, 23).

Application of casing layer, Day 35

On the straw surfaces various spore forms were found (Fig. 24). The density of the microbial populations was reduced compared to earlier stages but bacteria were still present within the straw cell walls (Fig. 25). The characteristic mycelium of the mushroom, Agaricus

Fig. 20 Day 21. SEM of fungal spores (F) on the straw surface. Note sporing actinomycetes (arrows). Bar 20 µm.
Fig. 21 Day 21. TEM of section of straw cell wall which is disintegrating due to erosion. Note actinomycete hyphae (arrow). Bar 10 µm.
Fig. 22 Day 21. TEM of actinomycete hyphae adjacent to straw cell wall. Note bud-like branch (arrow). Bar 1 µm.
Fig. 23 Day 21. SEM of straw cuticle severely eroded to expose underlying cells. Bar 30 µm.
Fig. 24 Day 35. SEM of straw surface with actinomycete spores (arrow), and Agaricus bisporus hypha (A) covered with calcium oxalate crystals. Bar 5 µm.
Fig. 25 Day 35. SEM of bacteria (arrows) embedded in eroded straw cell wall. Note lack of calcium oxalate crystals near growing tip of Agaricus bisporus hypha (A). Bar 10 µm.
Fig. 26 Day 35. SEM of area of straw cuticle showing little erosion and relatively few micro-organisms. Note absence of calcium oxalate crystals on Agaricus bisporus hypha (A). Bar 10 µm.
Fig. 27 Day 35. SEM of broken end of straw internode in phloem region. Note large number of organisms (O) and severe erosion of phloem. Bar 50 µm.

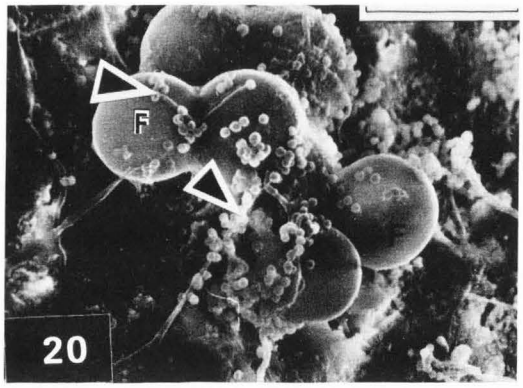
F
20

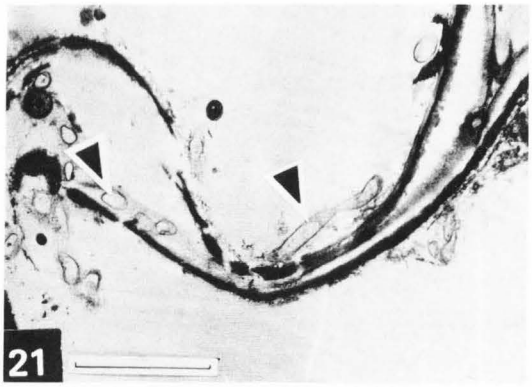
21

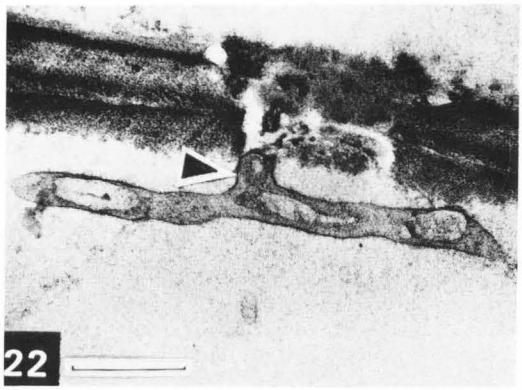
22

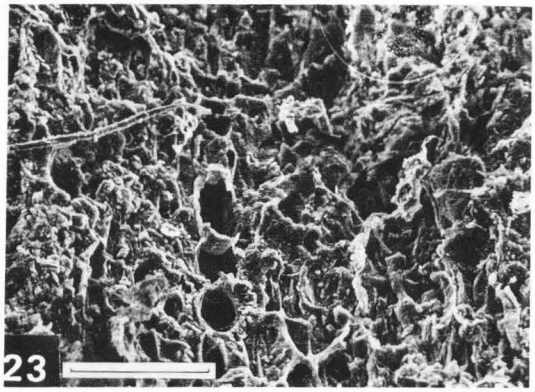
23

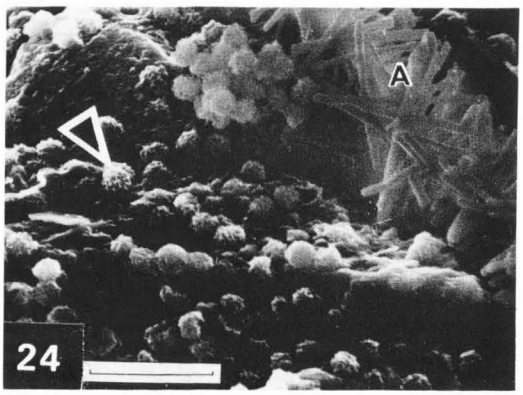
A
24

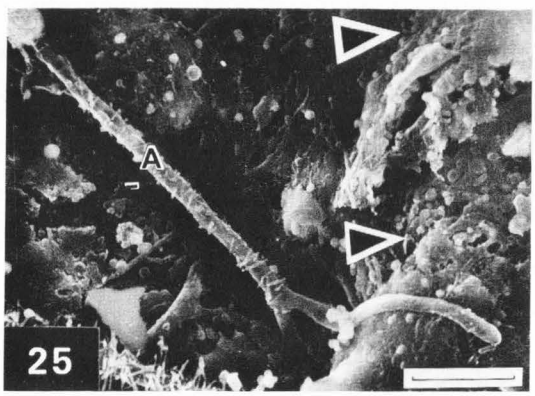
A
25

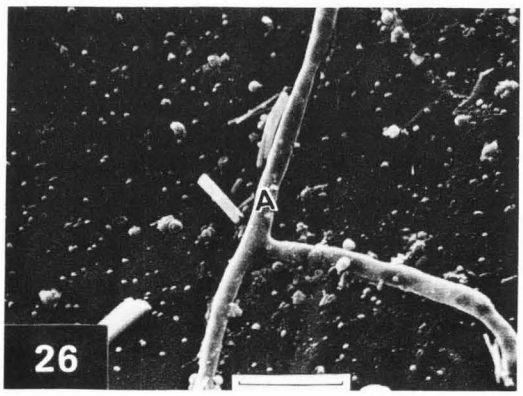
A
26

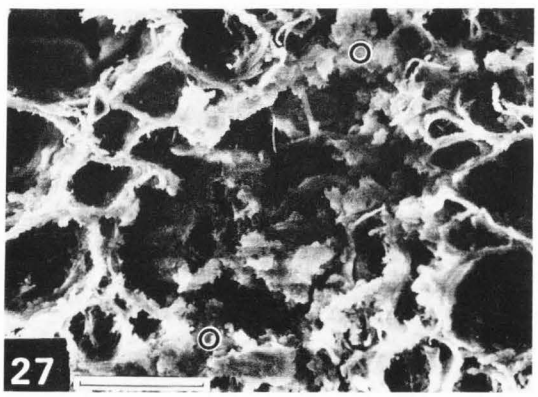
O
O
27

bisporus was found thinly distributed over the straw surface (Figs. 24, 25) but was not often found within the straw cells at this stage. Crystals, probably of calcium oxalate, were present at varying distances behind the hyphal tip (Figs. 24, 25). Degradation of the straw was non-uniform since areas were present which showed little evidence of microbial colonisation and degradation (Fig. 26). The broken ends of the straw showed severe erosion (Fig. 27).

First crop of fruiting bodies, Day 56

The microbial populations within the straw cells were further reduced. Many cells showed the presence of small unidentified hyphae (Figs. 28, 29). In many cases the straw surface erosion produced cracks within the structure (Fig. 30). The xylem tissue was often disintegrated leaving intact the secondary thickening and revealing the intravascular pits (Fig. 31). Separation of adjacent cells was found (Fig. 29).

End of fruiting, Day 112

The microbial population was small but still present within certain cells. The population contained many bacterial spores (Fig. 32). Various highly vacuolated hyphal-like cells (0.4-0.75 μm diameter) were present in the straw cells. These were found within the straw cells or associated with Agaricus hyphae (Fig. 32, 33). A. bisporus hyphae were present in about 30% of the straw cells. Many straw cells had lost their structural integrity (Figs. 32, 34). The mycelium formed a dense mat on the straw surface often completely covered with crystals (Fig. 35, 36), but nevertheless relatively undegraded areas were still present (Fig. 37) and the characteristic silicon bodies of the wheat epidermis were still present (Fig. 37). At this stage the jagged ends of the straw cells were relatively free of attached microorganisms (Fig. 38).

Development of mushroom fruit bodies

Rhizomorphs In compost part of the vegetative mycelium of Agaricus bisporus develops into aggregates of strands of hyphae termed rhizomorphs (Townsend, 1954). These strands were composed of a core of closely packed hyphae and an outer layer of narrow randomly arranged hyphae (Figs. 39, 40). These outer hyphae were often also encrusted with crystals (Figs. 35, 36). The central core hyphae were thick-walled and often highly vacuolated Fig. 41). In many of these cells electron dense crystalline bodies were found (Fig. 42). These crystals varied in size up to 1 μm diameter. They were bounded by a double membrane and had a repeating lattice structure (Fig. 42).

Primordium This is the earliest stage of mushroom development. At a size about 1-2 mm height a circular junction developed at the centre of the primordium separating it into two apparently identical regions (Fig. 43). As the primordium enlarges the two zones differentiate into cap and gill region and stipe region. The cap region developed two cavities in the annular zone (Fig. 44). The annular zone is the region of the developing gill tissue. Within this region basidial cells develop by swelling of hyphal tips to form club-shaped cells (Fig 45). These cells were densely packed with cytoplasmic contents. The arrangement of cells within this cavity is also shown by SEM (Fig. 46). The cell wall septa dividing these cells and those throughout the organism, contain structures termed dolipore septa (Beckett et al., 1974). A higher magnification view of these structures is shown in Fig. 47.

Gill tissue The mature gill tissue of Agaricus bisporus is composed of three regions: the trama, the sub-hymenium and the hymenium. These regions visualised by light microscopy and log magnification SEM (Figs. 48, 49, 50). The trama cells are elongated and run longitudinally down the centre of the gill from the cap to the edge of the gill (Figs. 49, 50). These cells are highly vacuolated. Branched subhymenial cells arose from the tramal cells at intervals along the gills. The hymenial region was composed of closely packed basidia with close wall to wall contacts. As the basidia enlarged they emerged from the surface of the gill (Fig. 51). The hymenial layer arose by complex branching and hyphal growth from the underlying sub-hymenial layer (Fig. 52). Serial section techniques were used to trace the origin of development of hymenial cells (Fig. 53).

Stipe tissue During mushroom development the stipe expands considerably raising the cap and gill tissue above the underlying substratum (Bonner et al., 1956). The expanding stipe consists of two main regions, the inner core and the main bulk, the outer stipe. The arrangement of hyphae varied in the different regions (Figs. 54, 55, 56, 57, 58, 59). The base consisted of

---

Fig. 28 Day 56. SEM of broken end of straw vascular bundle showing disorganised xylem vessel (X) and numerous small hyphae (arrows). Bar 50 μm.
Fig. 29 Day 56. TEM of section of straw cells with eroded lignified walls which are frequently detached from the middle lamella (*). Note hypha penetrating cell wall (black arrow) and small number of microbes (white arrows). Bar 5 μm.
Fig. 30 Day 56. SEM of straw surface exhibiting extreme erosion and cracking (arrows). Bar 100 μm.
Fig. 31 Day 56. SEM of straw vascular bundle eroded to reveal spiral thickening (S), intravascular pits of pitted elements (arrows) and sieve tubes (T). Bar 100 μm.
Fig. 32 Day 112. TEM of degraded straw vessel in longitudinal section showing wall separation (*) due to microbial activity. Note bacterial spores (white arrows), actinomycetes (black arrows) and Agaricus bisporus hypha (A). Bar 10 μm.

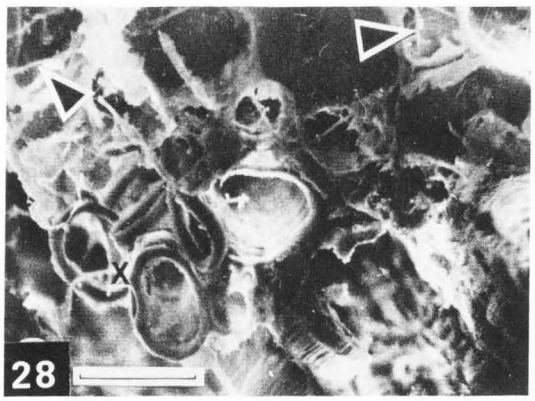
X
28

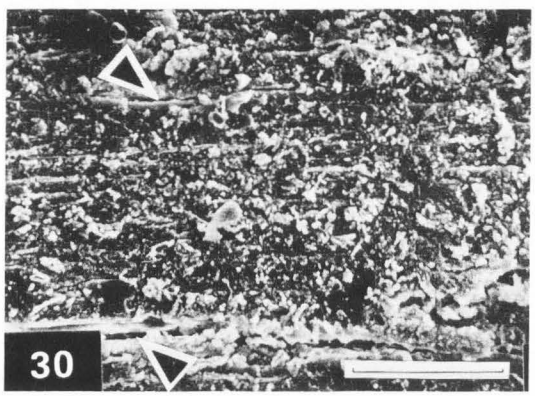
30

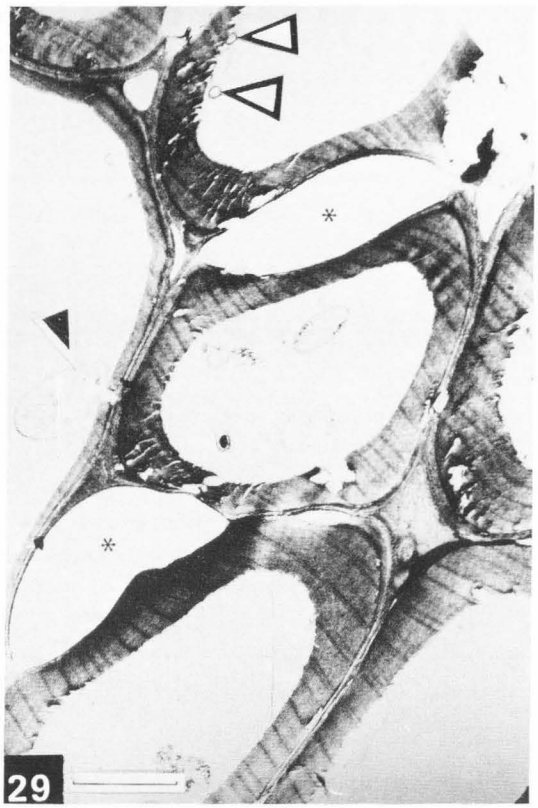
29

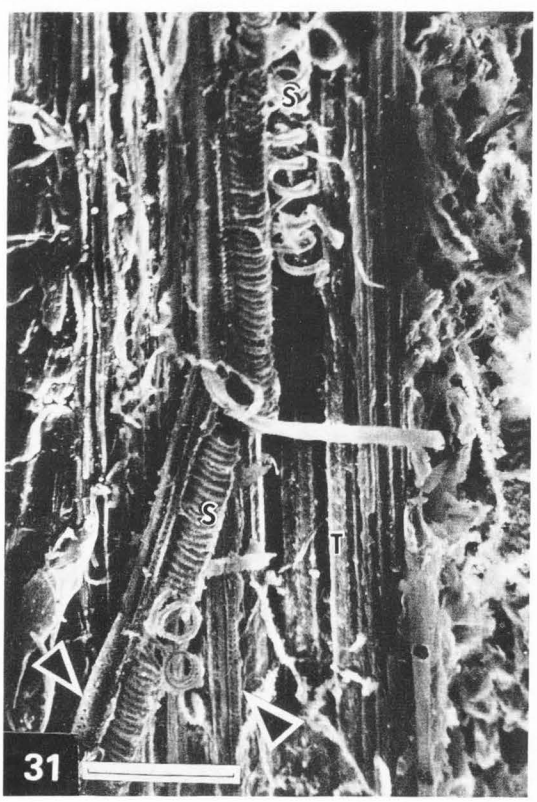
S
S
T
31


A
32

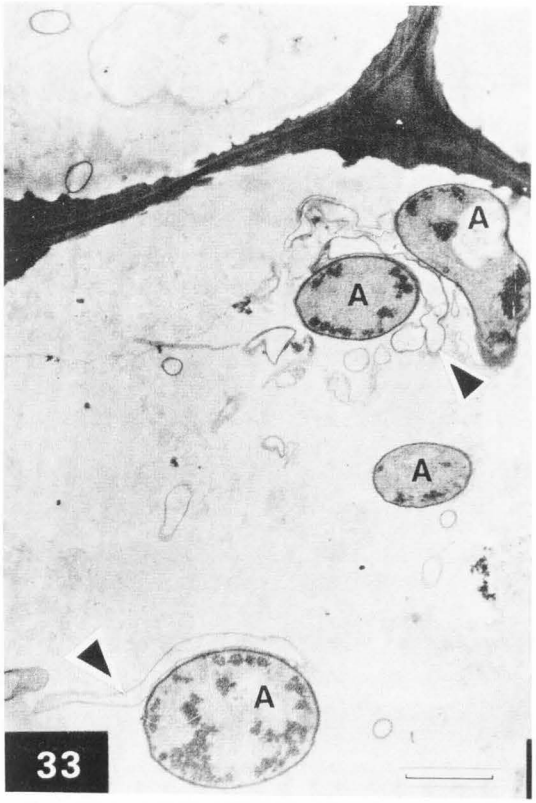
A
A
A
A
33

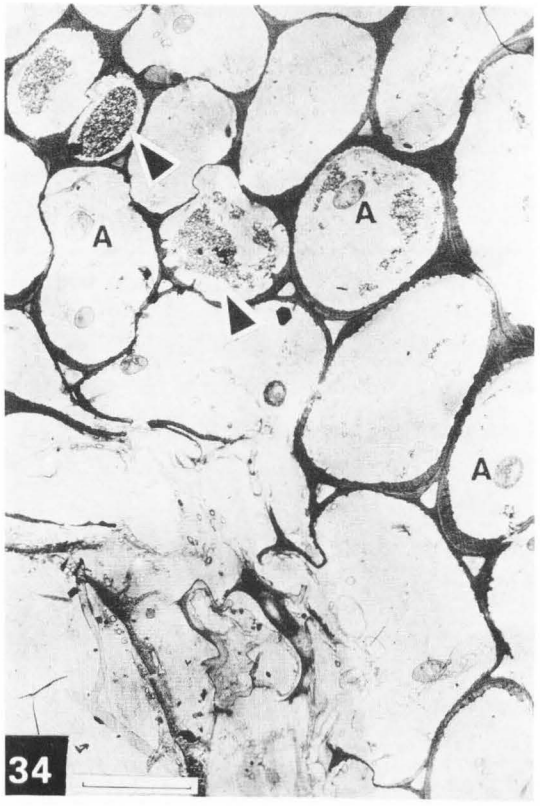
A
A
A
34

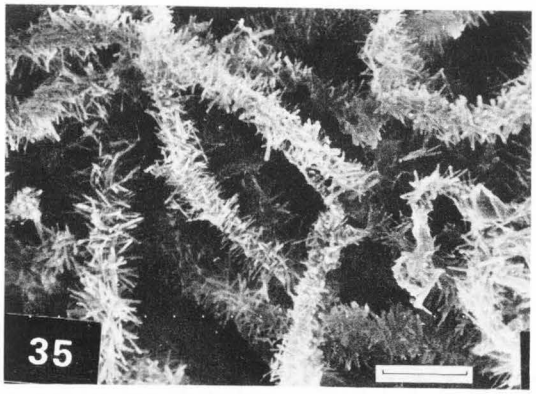
35

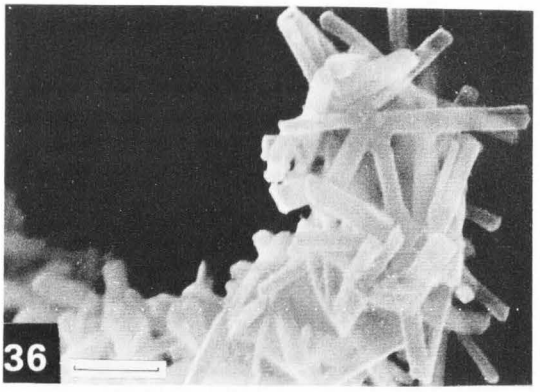
36

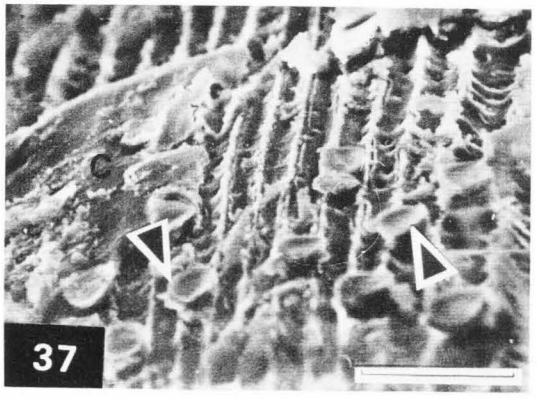
37

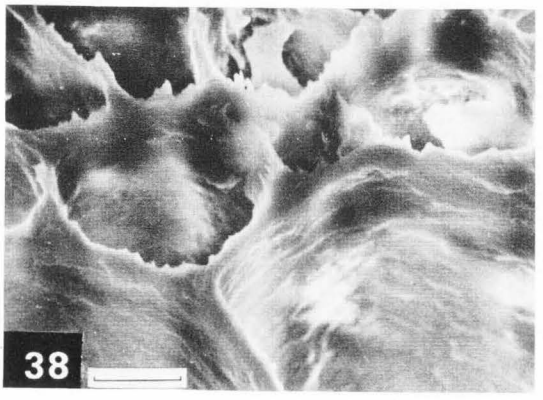
38

Fig. 33 Day 112. TEM of a degraded straw cell containing Agaricus bisporus hyphae (A) often in close proximity to vacuolated actinomycete cells (arrows). Bar 2 μm.
Fig. 34 Day 112. TEM of a transverse section of straw internode showing cell wall degradation leading to collapse in lower half of micrograph. Note Agaricus bisporus hyphae (A) and electron dense material (arrows). Bar 10 μm.
Fig. 35 Day 112. SEM of Agaricus bisporus mycelium, showing dense cover of calcium oxalate crystals right up to growing tip. Bar 20 μm.
Fig. 36 Day 112. Same as Fig. 35. Bar 2 μm.
Fig. 37 Day 112. SEM of the straw epidermis. Note area of undegraded cuticle (C) and surviving silica bodies (arrows). Bar 50 μm.
Fig. 38 Day 112. Broken end of straw internode showing jagged ends. Note lack of microbes at this stage of the crop. Bar 10 μm.

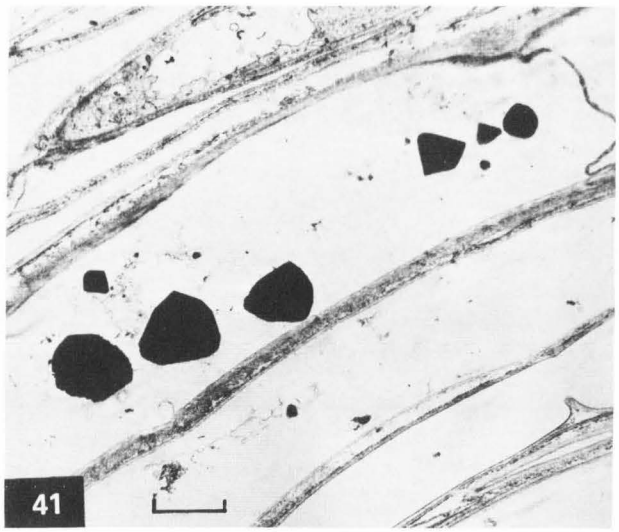

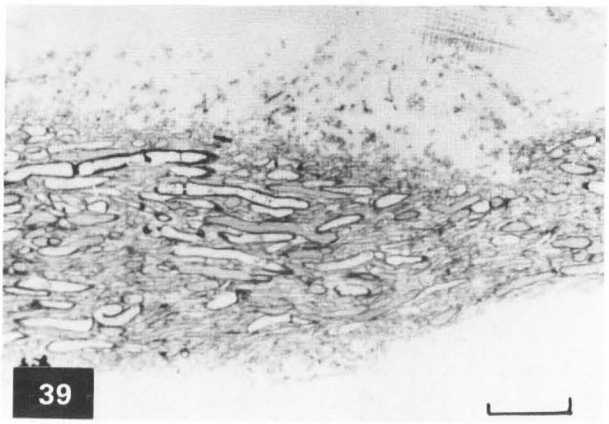

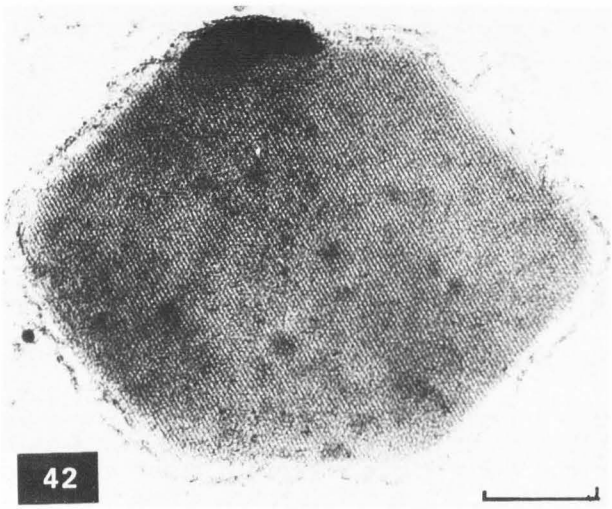

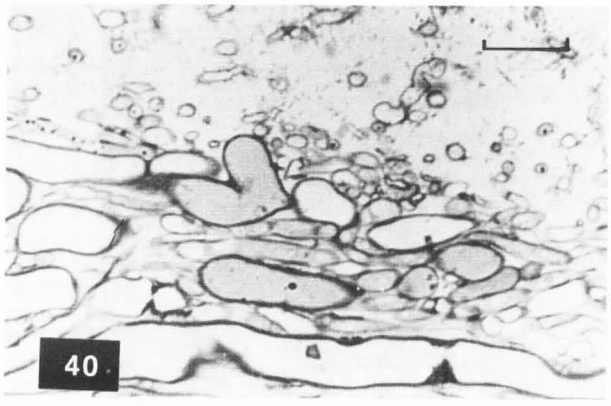

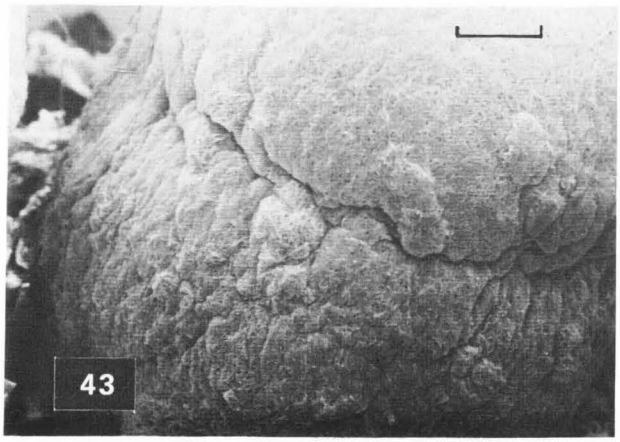

Fig. 39. Light micrograph of a longitudinal section of a rhizomorph of Agaricus bisporus stained with toluidine blue. Bar 100 μm.
Fig. 40. Light micrograph of a rhizomorph of Agaricus bisporus showing two types of hyphae. Bar 20 μm.
Fig. 41. TEM of highly vacuolated hyphae of the core of a rhizomorph. Some hyphae contain electron-dense crystalline bodies. Bar 10 μm.

Fig. 42. TEM of electron dense crystalline bodies showing double membrane and a repeating lattice structure. Bar 200 nm.
Fig. 43. SEM of a primordium showing the circular function developing at the centre. Bar 500 μm.

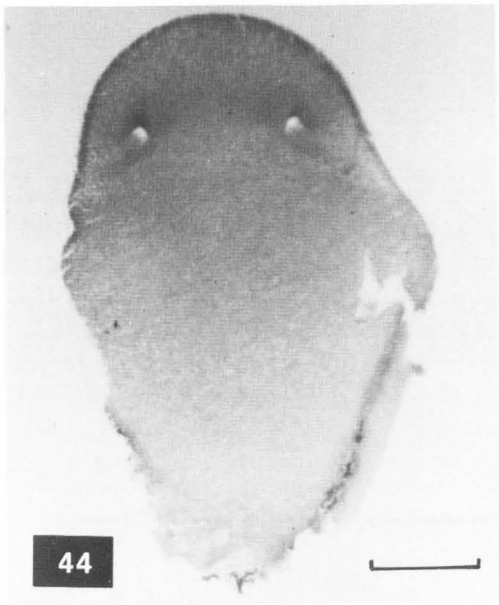
44

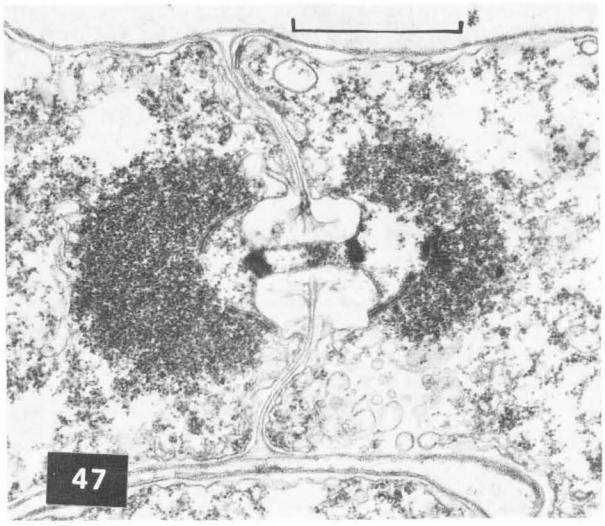
47

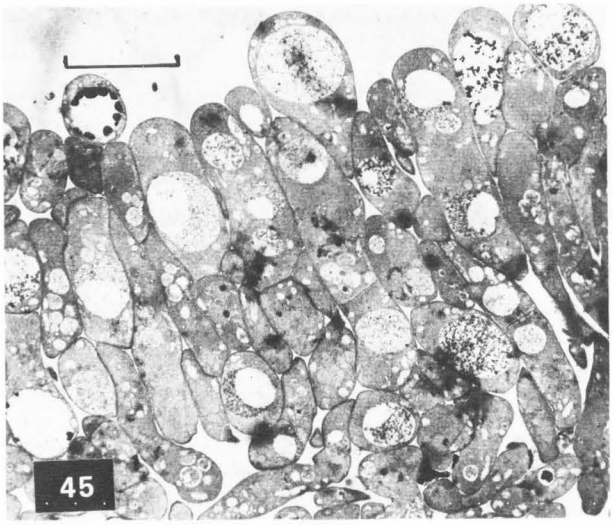
45

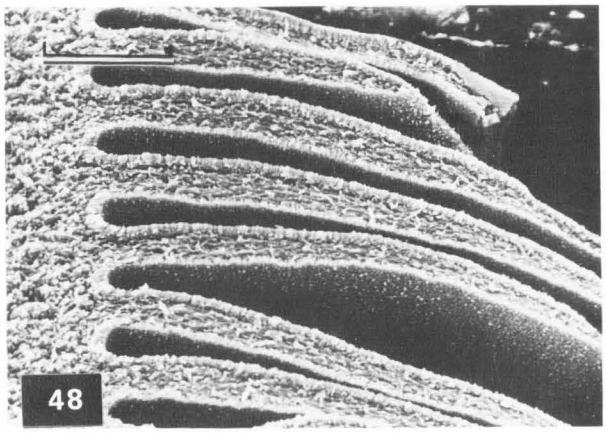
48

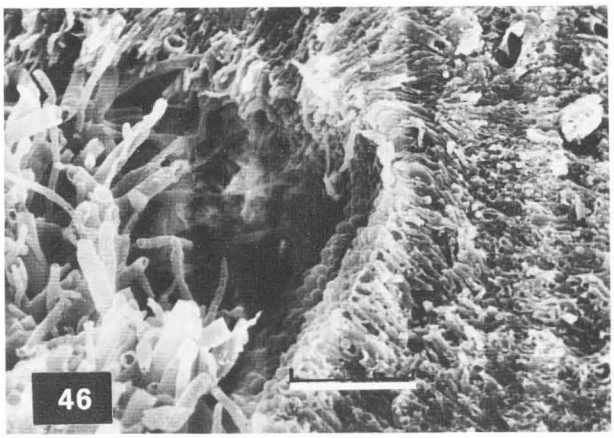
46

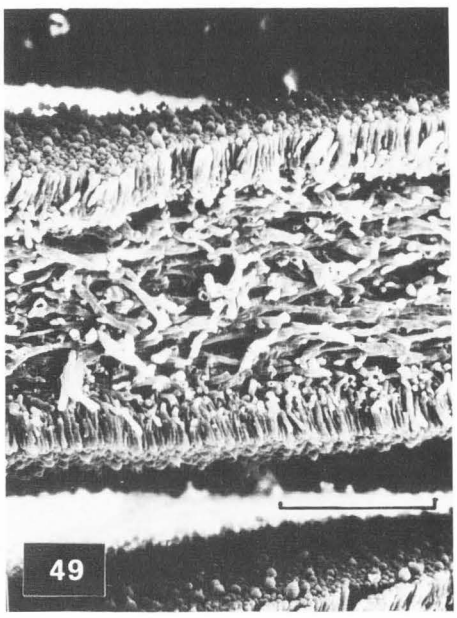
49

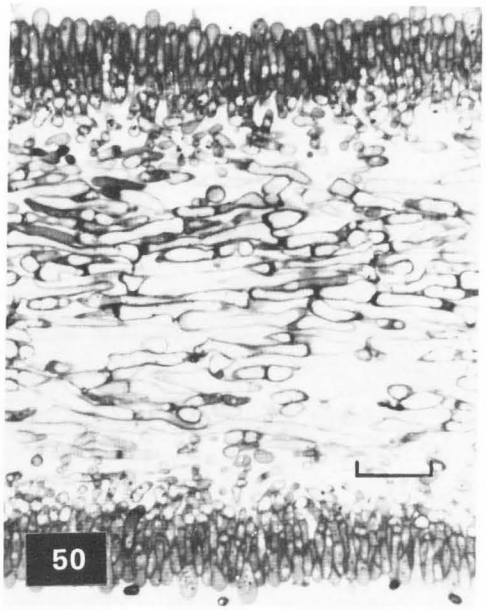

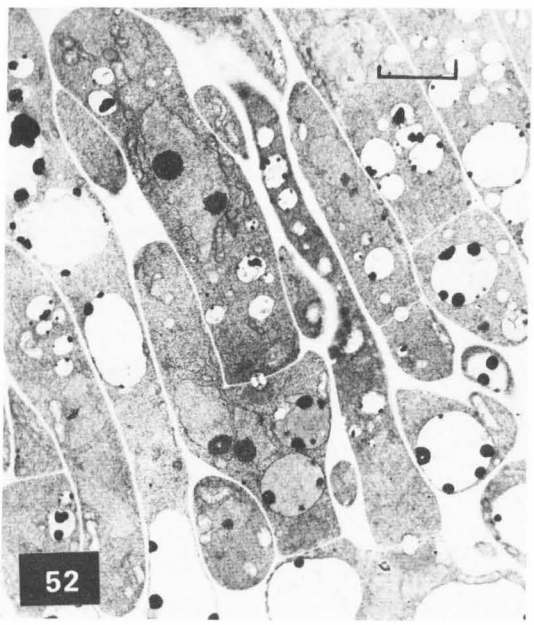

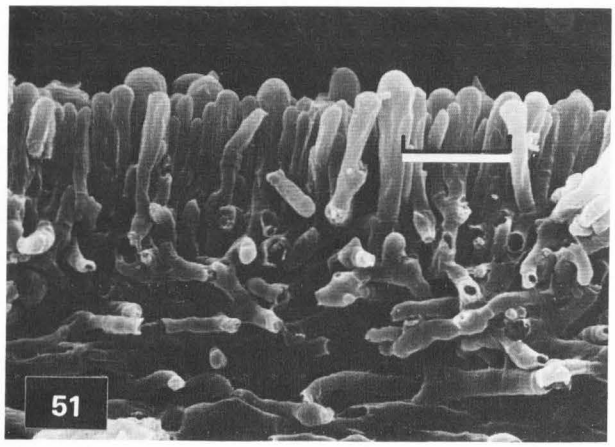

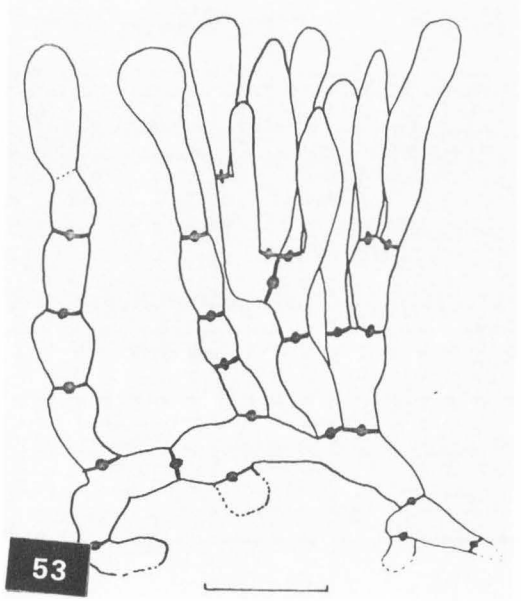

Fig. 44. Light micrograph of a complete section through a primordium stained with toluidine blue. Two annular cavities can be seen. Bar 1000 µm.
Fig. 45. TEM showing club shaped basidia. Bar 10 µm.
Fig. 46. SEM showing the arrangement of hyphal tips in the annular cavity. Bar 40 µm.
Fig. 47. TEM of a dolipore septum of a rapidly growing cell showing a perforate parenthosome cap surrounded by an outer cap consisting mainly of aggregates of ribosomes. Electron dense plugs can be seen in the pore of the septum. Bar 1 µm.
Fig. 48. SEM showing the mature gill. Bar 500 µm.
Fig. 49. SEM showing the mature gill tissue. Outer cell layer, hymenium, below this sub-hymenium, central layer of the trama. Bar 50 µm.
Fig. 50. Light micrograph of gill section showing dense cytoplasmic contents of hymenial cells. Bar 25 µm.
Fig. 51. SEM of the three regions of the gill tissue showing the complexity of branching in the sub-hymenial layer. Bar 20 µm.

Fig. 52. TEM of the hymenium and sub-hymenium of the mature gill showing branching patterns. Bar 2 µm.
Fig. 53. Diagram composed from serial section of gill tissue illustrating sub-hymenial branching. Bar 10 µm.

an irregular mass of closely packed thin hyphae (Figs. 54, 55). In the upper and mid-core regions there was a similar arrangement but the hyphae were packed more loosely and were vertically orientated (Figs. 56, 57). At the top of the stipe the inner region was randomly

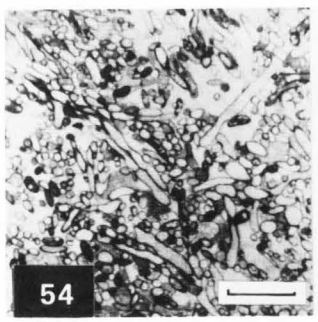

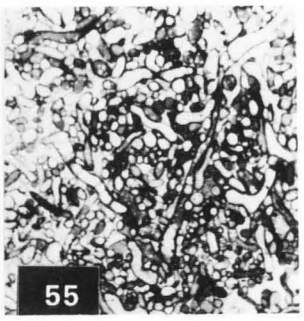

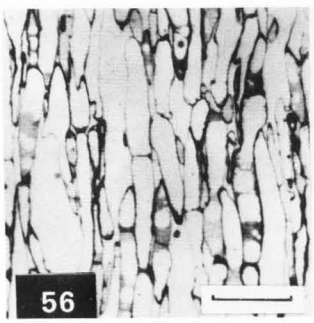

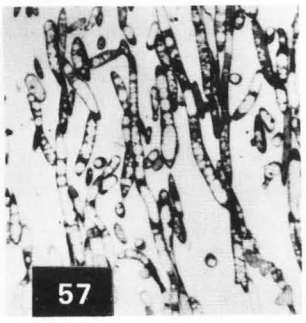

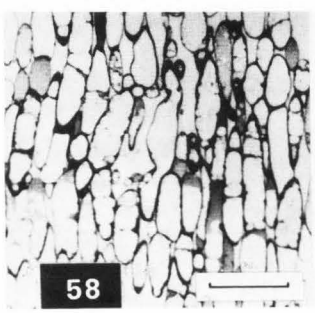

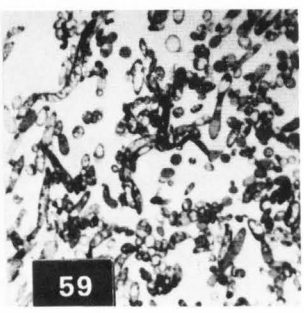

Figs. 54-59. Light micrographs of longitudinal sections of different regions of the stipe. Bar 50 μm. Fig. 54 - base outer; Fig. 55 - base inner, Fig. 56 - mid outer, Fig. 57 - mid inner; Fig. 58 - top outer; Fig. 59 - top inner.

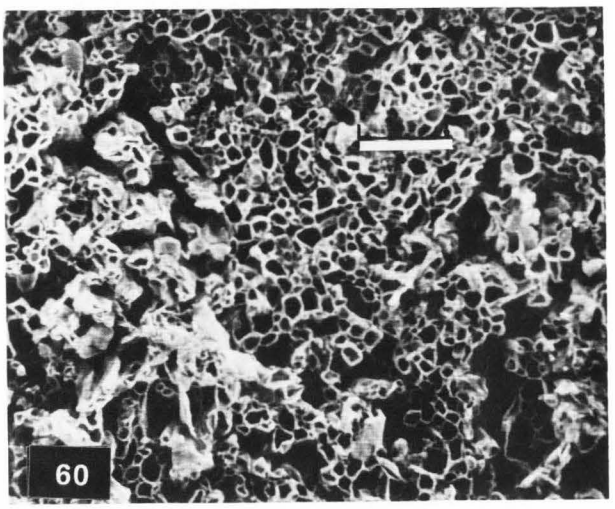

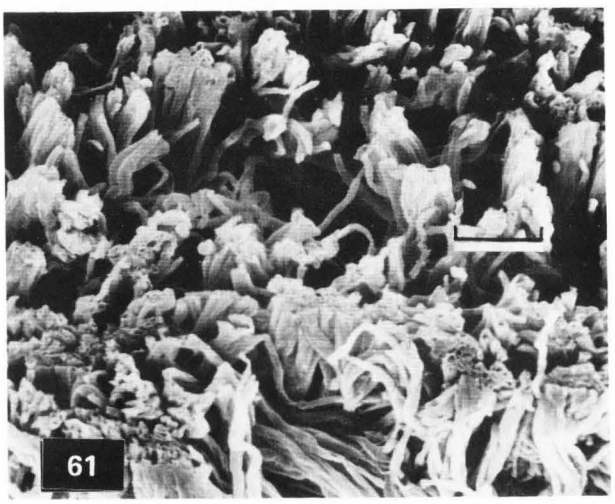

Fig. 60. SEM of a transverse section of the mid outer region of the stipe. Bar 100 μm.
Fig. 61. SEM of a transverse section of the mid core region of the stipe. Bar 100 μm.
Fig. 62. SEM showing the outer layer of hyphae on the surface of the stipe. Bar 100 μm.

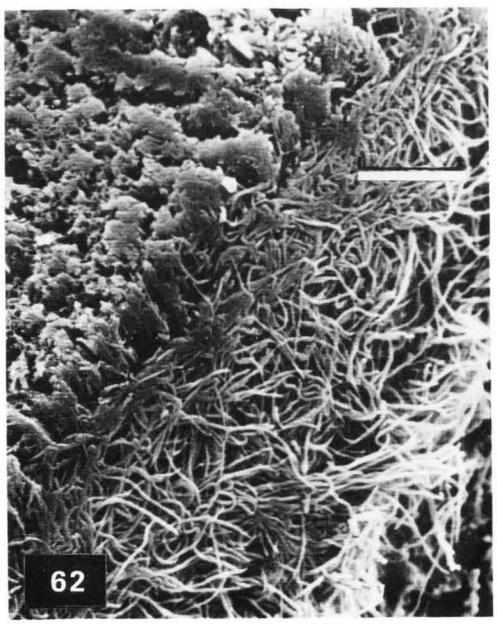

Figs. 63-65. TEMs of three different types of cell in the stipe. Bar 10 μm. Fig. 63 - cells of base and inner core; Fig. 64 - large vacuolated cells of outer stipe; Fig. 65- thin cells of extreme outer layer.
Fig. 66. TEM of glycogen rosettes in a stipe cell. Bar 1 μm.
Figs. 67-69. Light microscope autoradiographs of elongating cells of the stipe showing label all over the cells. Fig. 67 - Bar 60 μm; Fig. 68,69 - Bar 25 μm.

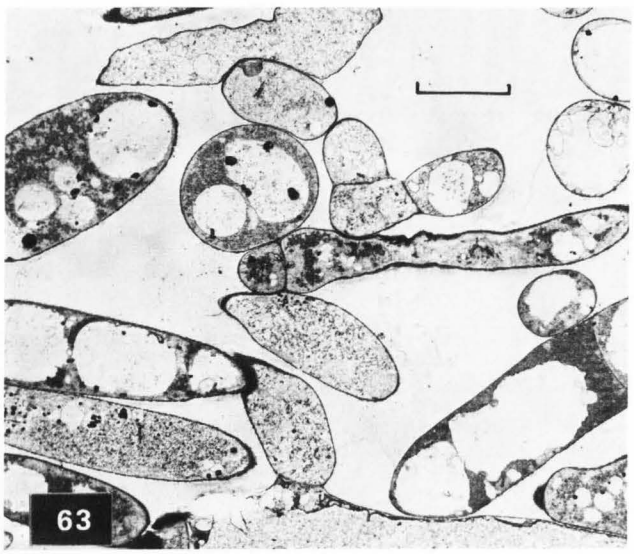
63

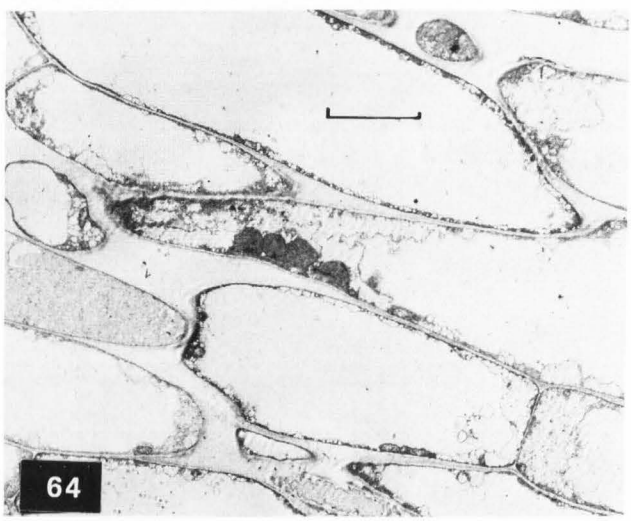
64

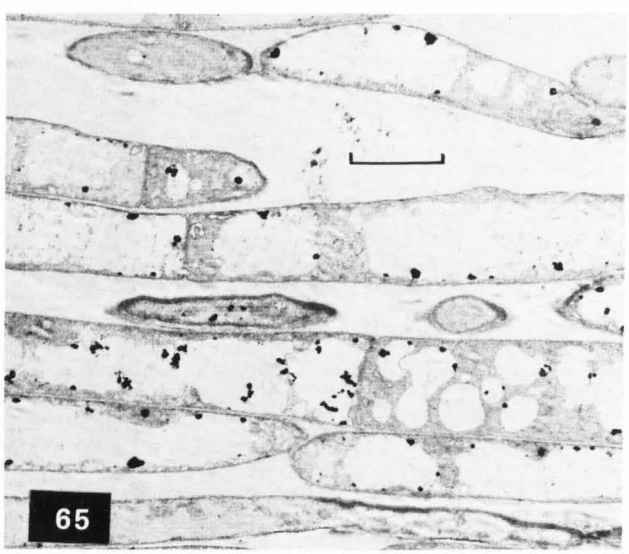
65

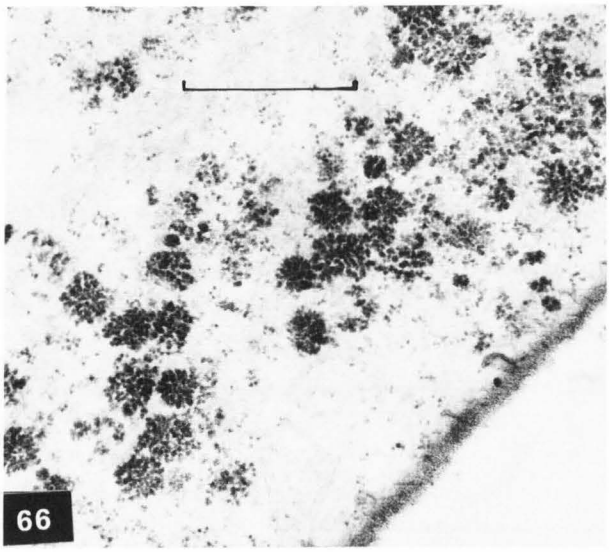
66

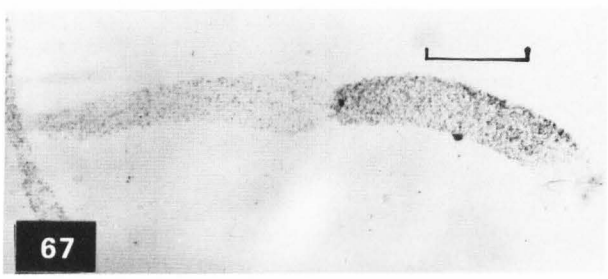
67

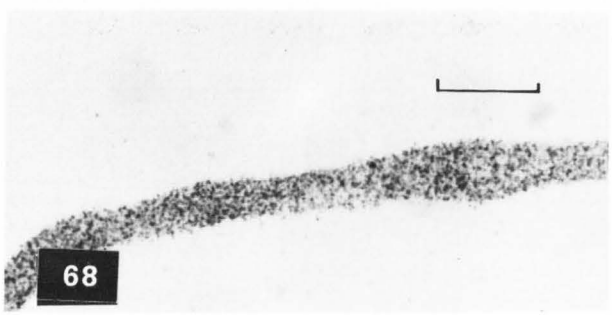
68

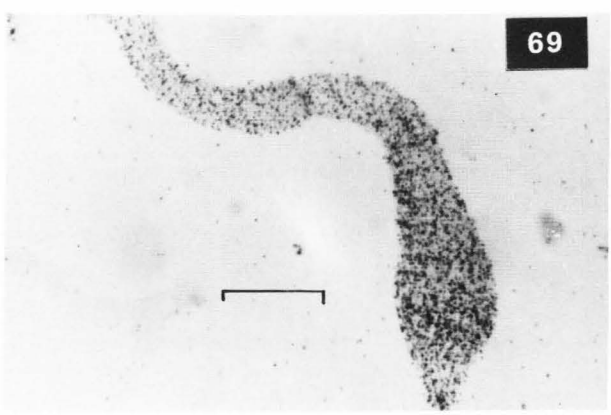
69

orientated but the outer region remained vertically orientated (Figs. 58, 59). SEM also showed differences in hyphal arrangement between mid-core and mid-outer region of the stipe (Figs. 60, 61).

On the outer stipe surface there was a layer of long slender hyphae arranged horizontally around the outer circumference (Fig. 62). TEM of the different cell types of the stipe revealed difference in their ultrastructural features (Figs. 63, 64, 65). The more slender cells of the base and inner regions of the stipe were rich in cytoplasm although there were some vacuoles in larger cells (Fig. 63). The larger elongated cells of the mid and upper outer regions of the stipe had sparse cytoplasm (Fig. 64). As the stipe expanded these cells elongated and the vacuoles became larger. The cells of the surface layers of the stipe were long and thin and contained electron dense granules (Fig. 65). Many of the stipe cells contained glycogen rosettes (Fig. 66). Stipe cells also contained similar protein crystals to those found in the rhizomorphs (Fig. 42).

Autoradiographic studies of stipe elongation

Incorporation of N-acetyl-D-[1-^{3}U] glucosamine was carried out with several stipes of fruit bodies during development. The pattern of incorporation varied from some cells with few silver grains to those with heavy incorporation (Fig. 67). The distribution of grains was all over the cell whether or not there was heavy labelling (Figs. 68, 69). In many hyphae the septa were also labelled (Fig. 70).

Labelled stipe cells were treated with KOH to remove the alkali-soluble outer wall layers and expose the underlying chitin microfibrils. The silver grain deposition appeared as small electron dense coils located all over the cell wall (Fig. 71). A higher resolution picture of this is shown in Fig. 72.

Autoradiography of thin sectioned stipe material showed that the added label was incorporated almost entirely into the cell wall-membrane region of the hyphae (Figs. 73, 74). The cell septum was also a site of incorporation into chitin (Figs. 75, 76). The label either concentrated on the tips of the ingrowing region or was distributed along the entire septum.

Discussion

These microscope studies of the substrate preparation and colonisation stages of mushroom cultivation and mushroom development have revealed information that could not have been achieved by other microbiological, biochemical or chemical techniques (Atkey and Wood, 1983). Although there was considerable information available on the microbial and chemical changes taking place during composting and cropping, the types of microbial attack on the plant tissue had not previously been visualised (Fermor and Wood, 1979). The microbial degradation patterns revealed show that these are comparable to those seen for lignocellulose biodegradation in other

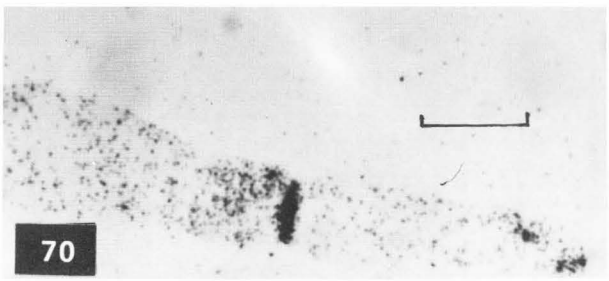

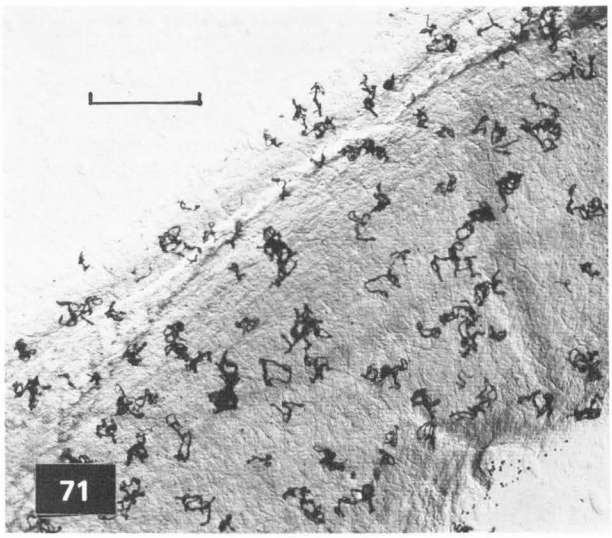

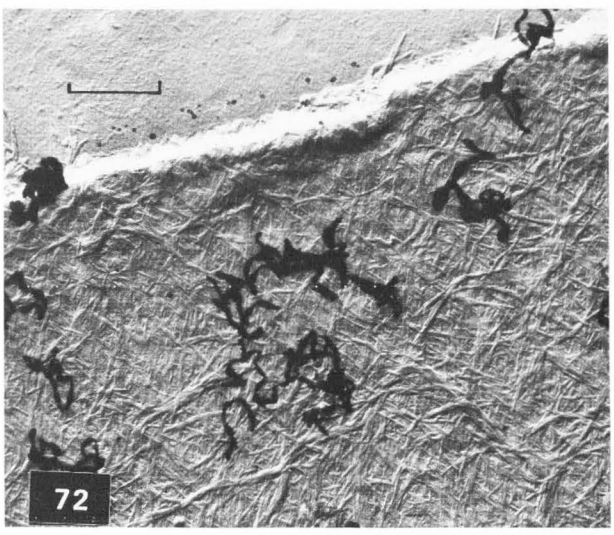

Fig. 70. Light microscope autoradiograph of elongating cells of the stipe showing labelled septa. Bar 20 μm.
Fig. 71. Transmission electron microscope autoradiograph of whole stipe cells treated with KOH to expose chitin microfibrils. Bar 1 μm.
Fig. 72. Electron microscope autoradiograph of a stipe cell showing chitin microfibrils and silver grain deposition. Bar 500 nm.

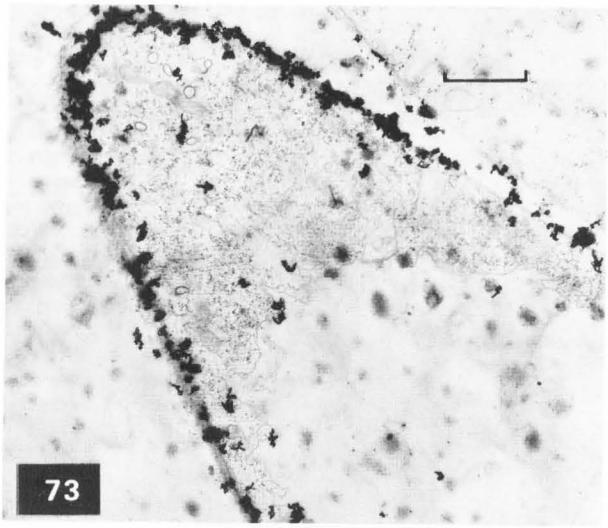

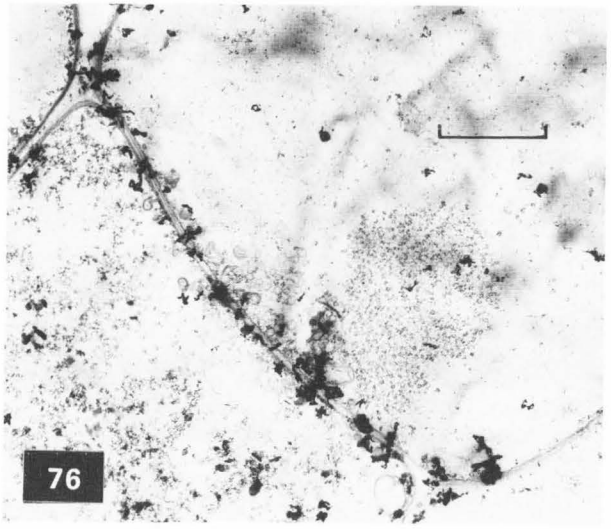

Fig. 73-74. Transmission electron microscope autoradiographs of thin sections of stipe cell. Label is almost entirely located on the cell wall and plasmalemma. Bar 2 μm.
Figs. 75-76. Transmission electron microscope autoradiographs of septa at different stages of growth. Fig. 75 shows two ingrowths from cell wall with label concentrated at the tips. Bar 2 μm. Fig. 76 shows higher resolution picture of a completed septum. Bar 500 nm.

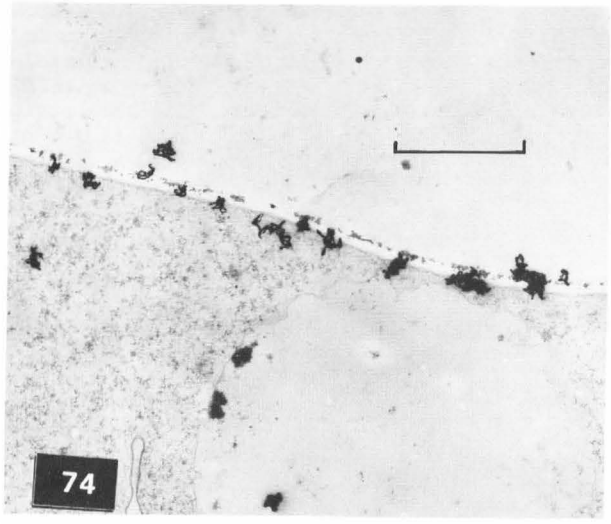

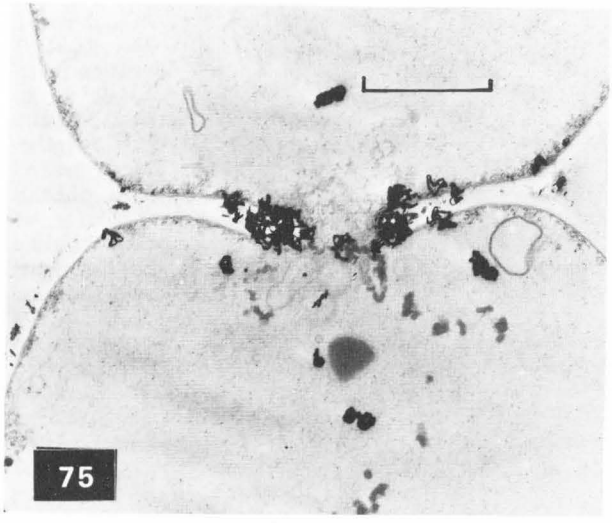

complex ecological environments such as the rumen (Akin et al., 1974; Akin, 1976; Dinsdale et al., 1978; Cheng et al., 1981) or in the preparation of silage (Moon and Henk, 1980).

Composting for mushroom cultivation is physiologically distinct in that a very wide range of mesophilic and thermophilic bacteria, fungi and actinomycetes can be isolated (Fig. 5). The microbial flora of the rumen is primarily anaerobic and mesophilic and comprises bacteria, protozoa and an anaerobic fungal flora. The major microbial flora of silage is a restricted one of mesophilic facultative anaerobic bacteria.

Various types of microbial attack on the straw can be seen with the electron microscope methods including concavities, tunnels and separation of fibres (Figs. 11, 13, 14, 16, 17, 21). The bacterial colonies showed evidence of being anchored to the walls by glycocalyx-like material (Costerton et al., 1978) (Figs. 11, 13) but further staining methods are required, such as the use of ruthenium red, to confirm this. Since the substrate (wheat straw) does not have large quantities of free water, during preparation the movement of bacteria to fresh colonisation sites may be restricted. This may in part explain the large variation in degradation observed between adjacent cells (Figs. 8, 11). Some degree of mixing is provided by the mixing and chopping action of the machinery used to turn the compost stack at intervals, but this may be insufficient to provide efficient spread of microorganisms.

The mode of attack of the microorganisms seemed to be initially on the straw epidermis and the cut ends (Figs. 4, 6, 9, 10, 12, 27).

A general pattern observed was that erosion of secondary thickening took place mostly on the parenchyma cells (Figs. 12, 16, 17), but later in the process there was attack on the vascular tissues (Fig. 29). Akin (1980) has observed similar differential attack by microorganisms degrading plant tissue in the rumen. This attack leaves the vascular thickening intact but separated from the surrounding tissue to leave a set of rings, spirals or fibres (Figs. 16, 17, 31).

The greatest density of vegetative microbes seemed to coincide with the middle stages of the composting process (day 7, day 14, Figs. 7, 11, 12, 13, 14, 18, etc.), but the variation in colonisation and degradation between individual plant cells (Fig. 37) observed indicates that more quantitative assessment is required to confirm this. Later in the composting and colonisation stages microbial spore forms were abundant (Figs. 15, 19, 32). This type of information would not be readily achieved by microbiological methods. Actinomycetes were found by TEM and SEM observation particularly at the later stages of the composting process (Figs 14, 15, 22, 28) and often formed spores on the straw surface (Figs. 20, 24). This observation is paralleled by the microbiological studies where it is known that a large actinomycete flora can be isolated at these stages (Fermor and Wood, 1979).

The mycelium of A. bisporus grew over the straw surface rapidly but was slower to colonise the internal parts (Figs. 23, 25, 26). By the end of the cropping process most of the straw was covered but only about 30% of the internal straw tissue contained hyphae of A. bisporus (Fig. 34). The microscope studies have not revealed what specific effects the mushroom mycelium has on the plant cell walls because of the previous intensive erosion and damage caused by the microbes present in the composting process (Fig. 30).

It is known that A. bisporus can degrade most of the plant biopolymers likely to be present in compost such as lignin, cellulose, hemicellulose and protein (Wood and Goodenough, 1977; Wood and Fermor, 1981; Wood and Leatham, 1983; Wood, 1984). In addition A. bisporus mycelium has been shown to be able to degrade and efficiently utilise microbial biopolymers from intact dead microbial cells as a nutrient source (Fermor and Wood, 1981; Sparling et al., 1982; Grant et al., 1984). The microbial biomass formed during composting has been shown to be capable of providing up to 10% of the total carbon nutrition of mushroom (Sparling et al., 1982). The observation that microbial cells decline in abundance in the straw cells (compare Figs. 11, 34, 38) correlated well with this observation of the nutritional capabilities of the mushroom. In addition the presence of moribund actinomycete hyphae (Fig. 33) close to the mushroom hyphae may indicate degradation of the former.

The mycelium on the straw surfaces produced a dense covering of needle-like crystals, probably of calcium oxalate (Piquemal et al., 1977) (Figs. 35, 36). The hyphae within the straw cells did not apparently have this covering (Figs. 33, 34). The function of this excretion of oxalic acid by mushroom mycelium is unknown.

In general the microscope studies have correlated well with previous microbiological and chemical studies of the processes. They have, however, revealed that the interactions of microorganisms with the substrate and each other are worthy of further study. Furthermore, although the microscope and microbiological studies both show that a large diverse microbial flora is responsible for the composting process, the identity of the organisms carrying out individual types of attack is unknown. Further work using immunocytochemical methods to identify the organisms 'in situ' will be required. This approach, combined with microbiological studies of straw breakdown using defined monocultures or mixed cultures of microorganisms isolated from composts may shed some further light on the identity and interactions of the complex flora of the composting process.

Earlier workers had used light microscopy to describe the morphogenesis of Agaricus fruit bodies (Atkinson, 1906, 1915; Hein, 1930). To correlate morphogenesis of the fruit body to biochemical events occurring both within the fruit body and within the underlying mycelium it is necessary to describe morphogenetic changes with better methods of microscopy (Craig et al., 1977(a) (b); Craig et al., 1979; Craig 1979). The fruit body of Agaricus and other basidiomycetes is a specialised differentiated structure designed for production and dispersal of large number of spores. Unlike plant meristematic cells, growth in fungi is controlled by regulating the growth of hyphal tips and subsequent branching from sub-apical compartments below the tip region (Burnett and Trinci, 1979).

Hyphal differentiation occurred even at the stage of the colonisation of vegetative mycelium into compost. Two types of hyphae developed which became organised to form mycelial strands or rhizomorphs (Figs. 39, 40). Fungal rhizomorphs are often formed by basidiomycetes and act as translocating organs.

Following the application of the casing layer and suitable environmental manipulation mushrooms are initiated as small aggregates of hyphae on the culture surface (Figs. 2, 3, 43). These aggregates enlarge and differentiate into two distinct regions (Figs. 43, 44). The upper region, the presumptive cap tissue, develops internally an annulus, the presumptive gill tissue (Fig. 44). The hyphae that develop within this annulus were cytologically distinct from the remainder of the primordial hyphae. The hyphal tips grow downwards forming the primordial gill tissue (Figs. 45, 46).

The mature gills of A. bisporus were highly organised and were composed of three regions: the trama, the sub-hymenium and the hymenium (Figs. 49, 50, 51). Basidial cells are formed in the hymenial layer (Figs. 52, 53). The basidia are formed by hyphal tips arising from complex branching patterns from the sub-hymenial cells (Niederpruem et al., 1971). This pattern has been referred to as the "candelabra" effect (Smith, 1966). This type of branching pattern can be traced by the use of serial section methods and an example is shown in Fig. 53.

A common feature of basidiomycete fungi is a complex structure formed between two hyphal cells at the cell-cell junction, called the dolipore septum (Beckett et al., 1974) (Fig. 47). The septa are characterised by a swelling around the central pore and a hemispherical perforate cap (the parenthosome) on each side of the pore. The structure of the dolipores of gill septa of Agaricus varied with position in the gill. Cell septa in the hymenium and tramal layers had the usual structure (Craig et al., 1977a; Craig, 1979) (Fig. 47).

The function of the stipe of mushrooms is to raise the developing fruit body to assist aerial dispersion of the spores. Manocha (1965) stated that there were only two types of stipe cell. Our evidence indicates that there are at least three distinct cell types in stipe tissue (Figs. 54, 55, 56, 57, 58, 59). These stipe cells differ greatly from the cells of the sub-hymenium, and hymenium of the gill (Figs. 50, 51) in that they are much elongated, and less closely packed (Figs. 60, 61). At the ultrastructural level these cells were more vacuolated than those of the gill tissue (Figs. 63, 64, 65). The large vacuolate cells of the core of the upper parts of the stipe are responsible for the bulk of elongation within that tissue (Craig et al., 1977a, b). Certain of the stipe cells contained glycogen rosettes (Fig. 66). These were present in both the expanded and non-expanded cells of the stipe. The glycogen content of Agaricus is known to increase during development from stage C to stage F (Fig. 2) (Hammond and Nichols, 1976). The results here do not indicate if this glycogen is being utilised as a carbohydrate reserve for fruit body construction as suggested for Coprinus cinereus (Blayney and Marchant, 1977). Stipe cells also contained electron dense bodies (Fig. 65) similar to those seen in the rhizomorph cells (Figs. 40, 41). These are similar to the protein structures found in other fungal cells (Armentrout and Maxwell, 1974; Mason and Crosse, 1975; Blayney and Marchant, 1977). No direct cytochemical or biochemical evidence is yet available as to the role of these crystals in basidiomycete fungi.

The upper stipe of basidiomycete fungi is known to elongate to a greater extent than the lower stipe (Bonner et al., 1956; Eilers, 1974; Cox and Niederpruem, 1975). Bonner et al. (1956) claimed that stipe elongation from A. bisporus after the 18 mm tall stage was due solely to cell elongation and not cell division. This conclusion was reached after taking measurements of cell length in premarked regions of the stipe before and after cell division. A similar technique was used by Craig et al. (1977b) to re-examine the work of Bonner et al. (1956). Evidence was obtained from both cell length measurement and autoradiography of elongating cells of the stipe that cell division did in fact occur in the upper stipe region. In agreement with the work of Bonner et al. (1956) it was found that the greatest length expansion occurred in the upper stipe region (Craig et al., 1977b). Evidence was obtained to show that stipe cells actively incorporated a radiolabelled chitin precursor, N-acetylglucosamine, to labelled material in the cell wall (Figs. 67, 68, 69). In addition labelled material was also found in the septa of cells of the upper stipe which must be synthesised during cell division (Fig. 70). N-acetylglucosamine is incorporated into the chitin of fungal cell walls by the action of the enzyme chitin synthase (Wood and Hammond, 1977). In vegetatively growing hyphae, chitin deposition is most active at the hyphal tip (Gooday, 1971). By contrast the stipe cells show a pattern of incorporation whereby label is distributed at several sites in the growing cells (Figs. 67, 68, 69, 70). This is also confirmed by electron microscope autoradiography of stipe cells treated with KOH to reveal chitin microfibrils. In these preparations silver grains are closely associated with the chitin microfibrils (Figs. 71, 72, 73). It is known that the chitin synthase system is located at the cell wall-membrane interface. Radiolabelled sectioned stipe tissue showed good evidence for the presence of an active chitin synthesising system in this region (Figs. 74, 75). The cell septa of stipe tissue of Agaricus form by centripetal growth as described by Hunsley and Gooday (1974) for Neurospora crassa. The heavy labelling of cell septa is good evidence for this mechanism in Agaricus (Figs. 76, 77).

These electron microscope studies have greatly aided the understanding of the cellular and biochemical processes which occur to form the final differentiated structure of the mushroom. They also indicate that a remarkable diversity of cellular interaction and development is required to produce a marketable crop of mushrooms. Knowledge of the structure and development of mushrooms will be of use in understanding the various processes which can occur in the post harvest biology of this rather unique crop species.

Acknowledgements

We are grateful to Mr Steve Matcham and Mr John Pegler for assistance with specimen preparation and electron micrography.

References

Akin DE. (1976). Ultrastructure of rumen bacterial attachment to forage cell walls. Appl. Environ. Microbiol. 31, 562-568.

Akin DE. (1980). Attack on lignified grass cell walls by a facultatively anaerobic bacterium. Appl. Environ. Microbiol. 40, 809-820.

Akin DE, Burdick D, Michaels GE. (1974). Rumen bacterial interrelationships with plant tissue during degradation revealed by transmission electron microscopy. Appl. Microbiol. 27, 1149-1156.

Armentrout VN, Maxwell DP. (1974). Hexagonal crystals in an ergosterol-free mutant of Neurospora crassa. Can J. Microbiol. 20, 1427-1428.

Atkey PT, Wood DA. (1983). An electron microscope study of wheat straw composted as a substrate for the cultivation of the edible

mushroom (Agaricus bisporus). J. Appl. Bact. 55, 293-304.

Atkinson GF. (1906). The development of Agaricus campestris. Bot. Gaz. 62, 241-264.

Atkinson GF. (1915). Morphology and development of Agaricus rodmanii. Proc. Am. Phil. Soc. 54, 309-342.

Beckett A, Heath IB, McLaughlin DJ. (1974). An Atlas of Fungal Ultrastructure, Longman, London.

Blayney GP, Marchant R. (1977). Glycogen and protein inclusions in elongating stipes of Coprinus cinereus. J. Gen. Microbiol. 98, 467-476.

Bonner JT, Kane KK, Levey RN. (1956). Studies on the mechanics of growth in the common mushroom, Agaricus campestris. Mycologia (N.Y.) 48, 13-19.

Burnett JH, Trinci APJ. (1979). Fungal Walls and Hyphal Growth. Cambridge University Press, Cambridge, UK.

Caro LG, van Tubergen RP, Klob JA. (1962). High resolution autoradiography . I. Methods. J. Cell Biol. 15, 173-188.

Cheng KS, Fay SP, Coleman RN, Milligan LP, Costerton JW. (1981). Formation of bacterial microcolonies on feed particles in the rumen. Appl. Environ. Microbiol. 41, 298-305.

Costerton JW, Geesey GG, Cheng KS. (1978). How bacteria stick. Sci. Am. 238, 86-95.

Cox RS, Niederpruem DS. (1975). Differentiation in Coprinus lagopus. II. Expansion of excised fruit bodies. Arch. Microbiol. 105, 257-260.

Craig GD. (1979). Morphogenesis in Agaricus bisporus. PhD Thesis, University of Nottingham, Nottingham, UK.

Craig GD, Newsam RS, Gull K, Wood DA. (1977a). Subhymenial branching and dolipore septation in Agaricus bisporus. Trans. Br. Mycol. Soc. 69, 337-344.

Craig GD, Gull K, Wood DA. (1977b). Stipe elongation in Agaricus bisporus. J. Gen. Microbiol. 102, 337-347.

Craig GD, Newsam RS, Gull K, Wood DA. (1979). An ultrastructural and autoradiographic study of stipe elongation in Agaricus bisporus. Protoplasma 98, 15-29.

Dinsdale D, Morris ES, Bacon JSD. (1978). Electron microscopy of the microbial populations present and their modes of attack on various cellulosic substrates undergoing digestion in the sheep rumen. Appl. Environ. Microbiol. 36, 160-168.

Eilers FI. (1974). Growth regulation in Coprinus radiatus. Arch. Microbiol. 96, 353-364.

Fermor TR, Wood DA. (1979). The microbiology and enzymology of wheat straw mushroom compost production. In "Straw Decay and its Effect on Disposal and Utilization" (Grossbard, E, ed.), John Wiley, New York, p. 105-112.

Fermor TR, Wood DA. (1981). Degradation of bacteria by Agaricus bisporus and other fungi. J. Gen. Microbiol. 126, 377-387.

Gooday GW. (1971). An autoradiographic study of hyphal growth of some fungi. J. Gen. Microbiol. 67, 125-133.

Grant WD, Fermor TR, Wood DA. (1984). Production of bacteriolytic enzymes and degradation of cell walls during growth of Agaricus bisporus on Bacillus subtilis. J. Gen. Microbiol. 130, 761-769.

Hammond JBW, Nichols R. (1976) Glycogen in Agaricus bisporus. Trans. Brit. Mycol. Soc. 66, 325-327.

Hein I. (1930). Studies on morphogenesis in Agaricus campestris. Am. J. Bot. 17, 882-915.

Hunsley D, Gooday GW. (1974). The structure and development of septa in Neurospora crassa. Protoplasma 82, 125-146.

Karnovsky MJ. (1965). A formaldehyde-glutaraldehyde fixative of high osmolarity for use in electron microscopy. J. Cell Biol. 27, 137-138.

Manocha MS. (1965). Fine structure of the Agaricus carpophore. Can. J. Bot. 43, 1329-1333.

Mason PJ, Crosse R. (1975). Crystalline inclusions in hyphae of the glaucus group of Aspergilli. Trans. Brit. Mycol. Soc. 65, 129-139.

Moon NT, Henk WG. (1980). Progression of epiphytic microflora in wheat and alfalfa silages as observed by scanning electron microscopy. Appl. Environ. Microbiol. 40, 1122-1129.

Niederpruem DJ, Jersild RA, Lane PL. (1971). Direct microscopic studies of clamp connection formation in growing hyphae of Schizophyllum commune. I. The Dikaryon. Arch. Microbiol. 78, 268-280.

Pegler J, Atkey PT. (1978). An economic method of tissue processing. Micron 9, 238.

Piquemal M, Belot L, Viala G, Latine JC. (1977). Influence de la composition du milieu de culture sur la biosynthese d'acide oxalique par le mycelium d'Agaricus bisporus. C. Rend. Acad. Sci. Ser D. 284, 741-744.

Polak-Vogelzang AA, Sampson RA, de Leeuw GTN. (1979). Scanning electron microscopy of Acholeplasma colonies on agar. Can. J. Micro. 25, 1373-1380.

Reynolds ES. (1963). The use of lead citrate at high pH as an electron opaque stain in electron microscopy. J. Biophys. Biochem. Cytol. 17, 208-212.

Smith AH. (1966). The hyphal structure of the basidiocarp. In: The Fungi. (Ainsworth, GC, Sussman, AS, eds.), Academic Press, London, 2, 151-177.

Sparling GP, Fermor TR, Wood DA. (1982). Evaluation of methods for measuring microbial biomass in composted wheat straw and the possible contribution of the biomass to the nutrition of Agaricus bisporus. Soil Biol. Biochem. 14, 609-611.

Spurr AP. (1969). A low viscosity epoxy resin embedding medium for electron microscopy. J. Ultrastruct. Res. 26, 31-43.

Townsend BB. (1954). Morphology and development of fungal rhizomorphs. Trans. Brit. Mycol. Soc. 37, 22-233.

Wood DA. (1984). Microbial processes in mushroom cultivation, a large scale solid substrate fermentation. J. Chem. Tech. Biotechnol. 34B, 232-240.

Wood DA, Hammond JBW. (1977). Inhibition of growth and development of Agaricus bisporus by polyoxin D. J. Gen. Microbiol. 98, 625-628.

Wood DA, Goodenough PW. (1977). Fruiting of Agaricus bisporus. Changes in extracellular enzyme activities during growth and fruiting. Arch. Microbiol. 114, 161-165.

Wood DA, Fermor TR. (1981). Nutrition of Agaricus bisporus in compost. Mush. Sci. 11, 63-73.

Wood DA, Leatham GF. (1983). Lignocellulose degradation during the life cycle of Agaricus bisporus. Fed. Eur. Microbiol. Soc. Microbiol. Lett. 20, 421-424.

Wood DA, Lynch JM, Rudd-Jones DR. (1984). Research and the mushroom industry. J. Roy. Ag. Soc. 145, 144-158.

Discussion with Reviewers

F.J. Ingratta: Do the authors feel that the microbial population functions solely in straw degradation or that their metabolic products have an impact on biochemical and physiological changes noted in the fungal mycelium?
Authors: Axenically fruited cultures of Agaricus give comparable yields to non-axenic cultures. The metabolic products could have several roles and experimentally it is not yet possible to distinguish these.

F.J. Ingratta: Is the lack of/or slow-colonization of the straw by the fungus a result of some fungal-bacterial antagonism?
Authors: Agaricus bisporus is an inherently slow growing fungus. The growth rates through compost are equivalent to those on most laboratory culture media suitable for fungi. Lack of colonization of certain parts of the straw tissue could be due to a variety of nutritional or cultural factors.

D.E. Akin: What is the cause of cuticle removal? Is it microbial in nature?
Authors: Direct proof as to the agent(s) responsible for cuticle removal cannot be easily obtained. Nevertheless, we feel that the ultra-structural evidence would indicate that the composting microorganisms are responsible.

D.E. Akin: Could some of the extreme damage (i.e. spiral rings of xylem) be from physical damage and not microbial damage?
Authors: The high incidence of release of such structures indicates that microbial damage is reponsible but since mechanical mixing is used during composting there could be a degree of physical damage.

E.M. Jasinski: Why was the radiolabelled N-acetylglycosamine injected into the stipe tissue rather than into the growing medium?
Authors: To ensure that sufficient activity was incorporated into the developing tissue. Addition to the medium would probably not have allowed sufficient label to incorporate.

E.M. Jasinski: Will the N-acetylglucosamine be metabolised to form chitin after injection? Can it be transported into the cells for chitin synthesis?
Authors: Evidence from the biochemistry of chitin synthesis in other fungi, including basidiomycetes indicates this compound is polymerised to chitin. It is also known that it can be transported into and between cells.

E.M. Jasinski: Is the apparent lack of calcium oxalate crystals within the cells due to TEM sample preparation?
Authors: Yes, this is a possibility.

E.M. Jasinski: Could the electron-dense crystalline bodies found in the rhizomorphs be calcium oxalate crystals?
Authors: We feel these are protein bodies because: (a) they resemble similar, better characterised structures, from other fungi; (b) calcium oxalate crystals would probably not show the type of fine structure seen for these crystals.

E.M. Jasinski: Is it possible that these crystals are protein crystals as suggested for the stipe cells? What is the probability of seeing crystalline protein occurring in nature within the mushroom?
Authors: The rhizomorph cells and the stipe cells both contained similar structures (see Figs. 41, 42, 65) which we think are protein crystals. Such crystals have been observed in several fungi.

E.M. Jasinski: In several cases the authors mentioned seeing structures within the straw cell from SEM. Did the authors cryofracture the straw sample to see inside the cells?
Authors: No cryofactures were carried out. Straw interiors were revealed by splitting the straw longitudinally or by razor cutting to observe the ends in transverse section.

F.J. Ingratta: The follwoing references are relevant to the topic of this paper:

Evans HJ. (1959). Nuclear behaviour in the cultivated mushroom. Chromosoma 10, 115-135.

Michalenko GO, Hohl HR, Rast D. (1975). Chemistry and architecture of the mycellar wall of Agaricus bisporus. J. Gen. Microbiol. 92 (2) 251-262.

Oliver JM, Guillaumes J. (1976). Etude ecologique des composts de champignonnient I. Evolution de la microflora pendant l'incubation. Ann. Phytopath. 8 (3), 283-301.

Hayes WA. (1968). Microbiological changes in composting wheat straw / horse manure mixtures. Mushroom Sci. 7, 173-186.

Fergus CH. (1978). The fungus flora of compost during mycelium colonization by the cultivated mushroom Agaricus brunnescens, Mycologia 70, 636-644.

Flegler SL, Warper GR, Fields WG. (1976). Ultrastructural and cytochemical changes in the Basidiomycete dolipore septum associated with fruiting. Can. J. Bot. 54, 2244-2253.

Authors: Thank you.